Charles University in Prague

Faculty of Mathematics and Physics

MASTER THESIS

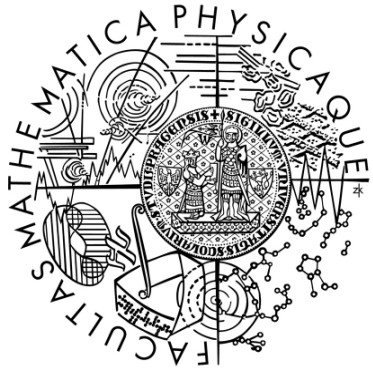

Peter Zalom

Regulation of intracellular pH in yeast - influence of selected transport proteins

Institute of Physics of Charles University

Supervisor of the master thesis: RNDr. Roman Chaloupka Ph.D.

Study programme: Physics

Specialization: Biophysics and Chemical Physics (FBCHF)

Prague 2011

Acknowledgements

I would like to thank RNDr. Roman Chaloupka, Ph.D. for his patient supervising and for comprehensive and constructive corrections of my master thesis. All the genetic manipulations were performed in Institute of Physiology AS CR, in the department of membrane transport, my thanks go especially to Mgr. Lýdia Marešová, Ph.D. and RNDr. Hana Sychrová, DrSc.

For all the support in times, when nothing seemed to fit, THANK YOU to my family, friends, to our good laboratorian Iva and especially to Peťa.

The dog trots freely in the street
and sees reality
and the things he sees
are bigger than himself
and the things he sees
are his reality

L. Ferlinghetti

I declare that I carried out this master thesis independently, and only with the cited sources, literature and other professional sources.

I understand that my work relates to the rights and obligations under the Act No. 121/2000 Coll., the Copyright Act, as amended, in particular the fact that the Charles University in Prague has the right to conclude a license agreement on the use of this work as a school work pursuant to Section 60 paragraph 1 of the Copyright Act.

In Prague 15. 4. 2011

Table of contents

Název práce: Regulace vnitřního pH kvasinek - vliv vybraných transportních proteinů

Autor: *Peter Zalom*

Katedra (ústav): *Fyzikální ústav Univerzity Karlovy*

Vedoucí diplomové práce: *RNDr. Roman Chaloupka, Ph.D.*

e-mail vedoucího: r*oman.chaloupka@mff.cuni.cz*

Abstrakt: Intracelulární pH ovlivňuje téměř všechny biochemické procesy v kvasinkách. Regulace cytosolického pH zahrnuje funkci mnoha transportních proteinů. Vliv vybraných sodných transportérů na cytosolické pH byl zkoumán u dvou druhů kvasinek: *Saccharomyces cerevisiae* a *Zygosaccharomyces rouxii* včetně divokých kmenů a mutantů s ovlivněným transportem sodíku. Měření cytosolického pH a pufrační kapacity bylo provedeno za použití fluorescenční sondy pHluorin - pH citlivého derivátu zeleného fluorescenčního proteinu. Bylo porovnáno několik postupů pro kalibraci fluorescenční odezvy pHluorinu na cytosolické pH. Byla prokázána důležitost korekce pro získaní správných kalibračních křivkek. Bylo zjisteno, že cytosolické pH je ovlivněno transportním proteinem Nha1 jak v *S. cerevisiae*, tak i v *Z. rouxii*, ale ne transportérem Sod2-22 přítomným v *Z. rouxii*. Bylo prokázáno, že pufrační kapacita cytosolu klesá v přítomnosti glukózy ve všech studovaných kmenech.

Klíčová slova: *Saccharomyces cerevisiae*, *Zygosaccharomyces rouxii*, pHluorin, cytosolické pH, transportéry sodíku

Title: *Regulation of intracellular pH in yeast - influence of selected transport proteins*

Author: *Peter Zalom*

Department: *Institute of Physics of the Charles University*

Supervisor: *RNDr. Roman Chaloupka, Ph.D.*

Supervisor's e-mail: r*oman.chaloupka@mff.cuni.cz*

Abstract: Intracellular pH affects nearly all biochemical processes in yeast, the processes regulating the cytosolic pH includes function of many transport proteins. In this work, the impact of selected sodium transporters on cytosolic pH has been studied in two yeast species: *Saccharomyces cerevisiae* and *Zygosaccharomyces rouxii* including wild-type and mutants with affected sodium transport. Measurements of cytosolic pH and buffering capacity have been performed using fluorescent protein probe pHluorin – a pH sensitive derivate of green fluorescence protein. Several procedures for calibration of pHluorin fluorescence response have been compared and the importance of a proper correction of the calibration curve has been demonstrated. It has been shown that cytosolic pH is influenced by the function of Nha1 transport protein in *S. cerevisiae* as well as in *Z. rouxii* but not by Sod2-22 transporter in *Z. rouxii*. It has been demonstrated that the buffering capacity of cytosol decrease in the presence of glucose in all strains studied.

Keywords: *Saccharomyces cerevisiae*, *Zygosaccharomyces rouxii*, pHluorin, cytosolic pH, sodium transporters

1. General introduction

Since a huge variety of processes maintaining life is coupled to the pH homeostasis, it is truly of great importance to determine processes influencing intracellular pH. Using pHluorin, a derivative of green fluorescence protein, we were able to quantify cytosolic pH in *Saccharomyces cerevisiae* and for the first time also in *Zygosaccharomyces rouxii*.

Our interest was aimed at the interdependence between cytosolic pH and alkali-metal homeostasis. For this purpose, mutants with deleted gene *nha1* were prepared for both yeast species. In the case of *Zygosaccharomyces rouxii*, also mutants with deleted *sod2-22* were used. Both genes were expected to influence cytosolic pH.

In the following text, a brief overview about pH homeostasis in the whole cell is given. Then, available results on cytosolic pH are discussed. At the end, we give a brief overview about alkali-metal homeostasis in yeast.

1.1. Yeast as model organism

Yeast is eukaryotic unicellular microorganism classified in the kingdom *fungi*. It is related to higher eukaryotes with a number of homologous genes shared together. Nevertheless, this is only one of the several reasons, why yeast has emerged as an important model organism. We briefly summarize the reasons now:

1. Compared to higher eukaryotes, yeast posses only a small and simply organized genome. The sequence of *Saccharomyces cerevisiae* for example contains about 12000 kilobases defining 6275 genes organized in 16 chromosomes [1].

2. Fully sequenced genome of selected yeast species allows easy deletion or addition of new genes [2].

3. Evolutionary relationship to other higher eukaryotic organism enables to extrapolate the results. It is for example estimated that yeast shares about 23% of its genome with mammalian cells [1].

4. Yeast cells are eukaryotes sharing most of the important inner cell structures with plants and animals. Hence, yeast cells are similar to higher eukaryotes in the cell structure and physiological processes [3].

5. The size, generation time and accessibility of yeast make it an easy to handle tool for phenotypic studies of genetic mutations [4].

6. Yeast research is economically favoured because of its established use in industry.

To study interdependence between cytosolic pH and alkali metal homeostasis we have used *Saccharomyces cerevisiae* and *Zygosaccharomyces rouxii* as model organisms. The second one is known for its ability to grow under conditions of high salt and/or glucose concentration. Both yeast species are closely related and belonged to the same genus until 1983, when Barnett et al. reclassified *Zygosaccharomyces rouxii* to its current name [5].

Since fully sequenced genomes for both yeast species are available, a common ancestor and phylogenetic tree including *Saccharomyces cerevisiae* and *Zygosaccharomyces rouxii* could be determined (see figure 1). Beside of relative close genetic relationship, there is a growing evidence that the ancestor of *Zygosaccharomyces rouxii* did not undergo the duplication of its entire genome (whole genome duplication, WGD) as it was the case of *Saccharomyces cerevisiae* ancestor [6,7].

For both yeast species, there are experimental data available connecting specific gene mutations with their phenotypic expression. Fully sequenced genome [1] of *Saccharomyces cerevisiae* enabled identification of membrane proteins involved in pH and alkali-metal homeostasis [8]. To date, there were several data published on organelle-specific pH (including cytosolic, mitochondrial and vacuolar pH) [9-12].

In the case of *Zygosaccharomyces rouxii*, there were genes identified, which are connected to in pH and alkali metal homeostasis, but no experimental data on cytosolic pH were published so far. On the other hand, several studies of alkali-metal transporters were performed [7,13,14].

Taken together, *Saccharomyces cerevisiae* is the more explored yeast species (different strains, transport kinetics for several transporter systems, different experimental methods). Beside this, our knowledge about participation of alkali-metal homeostasis in cytosolic pH is limited only on *Saccharomyces cerevisiae* [12]. Thus, obtaining of experimental data on cytosolic pH in *Zygosaccharomyces rouxii* helps to improve our knowledge about pH homeostasis in yeast species different from *Saccharomyces cerevisiae*. Choosing both, *Zygosaccharomyces rouxii* and *Saccharomyces cerevisiae,* enabled us also comparison of both organism almost directly, because experimental employed techniques varied only slightly for both (see section Material and methods). Subsequently, we were also able to verify the reliability of experimental methods used previously [9-12].

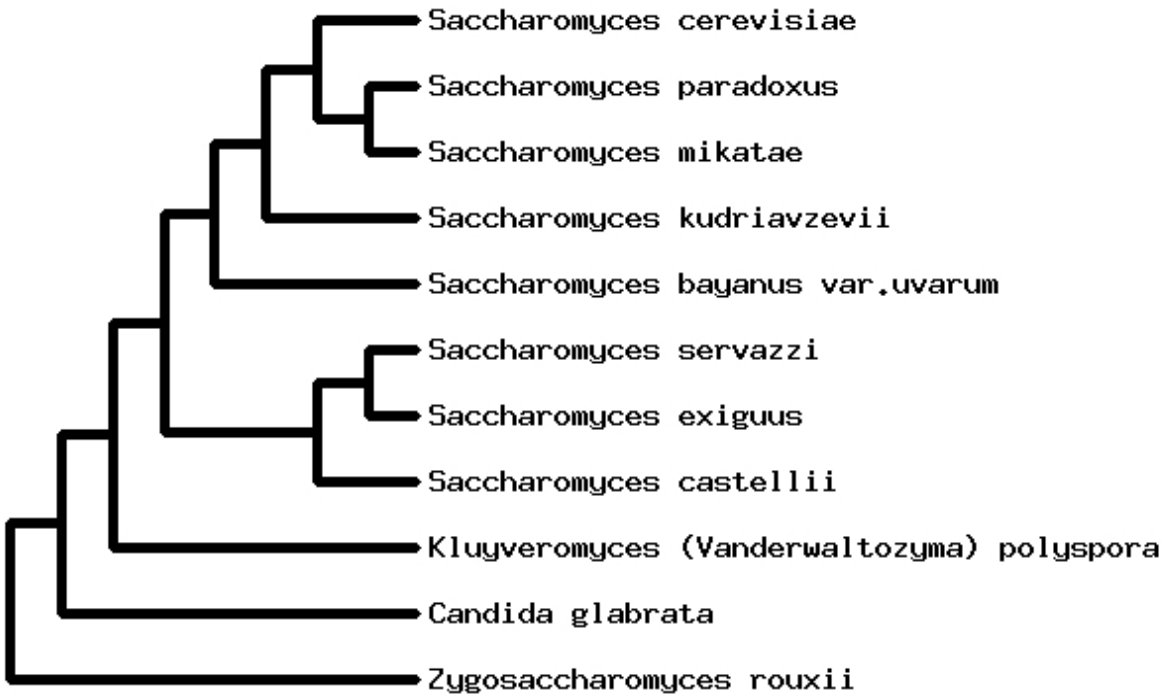

Figure 1 Phylogenetic tree of selected yeast species (an extract from phylogenetic tree published on the web site of Genolevures consortium, access in February 2011).

1.2. pH homeostasis in yeast

Living organism can adapt to a variety of stressful environments such as high or low temperatures, high or low osmotic pressures, environments containing oxidative stressors and weak organic acids [11]. Maintaining optimal life conditions is closely related to pH homeostasis, because it affects nearly all important biochemical processes:

1. Transport of nutrients across the plasma membrane is based on correctly adjusted pH gradients inside the cells [15-17].

2. The ionization states of acidic and basic amino acid side-chains depend on the value of intracellular pH. Thereby, pH influences the structure, solubility and activity of enzymes [18].

3. The actual size of pH affects NAD^+/NADH equilibrium. Thus, redox state of cells is influenced by pH [19].

4. Low pH inside the yeast vacuole is required to allow correct function of degradative enzymes [9].

5. Vesicle trafficking is reported to be regulated by pH [9].

6. Protein folding depends on a proper pH value [20].

7. Growth of yeast has been shown to correlate with rapid changes of cytosolic pH [11] and a possible regulatory pathway involving cytosolic pH as a second messenger has been proposed [21].

Because eukaryotic cells (including yeast) consist of several compartments, different pH values in cell organelles can be achieved. From this reason, whenever it is possible, we will make use of organelle-specific values of pH. In the case of averaging over the whole cell structure, we will use the term intracellular pH. To date, reliable experimental data are available on cytosolic, mitochondrial and vacuolar pH [9-12].

Before summarizing experimental data on pH homeostasis in yeast, we stress out two problematic points. First, there is a controversy about the accuracy of absolute values, which seem to depend on experimental techniques used [11]. Second, living cells are dynamic systems and hence, pH is not an static parameter, it rather depends on selected environmental parameters [11]. For example, addition of glucose to yeast deprived of energy sources causes a rapid change of cytosolic pH [10,11].

Nevertheless, relative differences of pH between several organelles are reported to be preserved generally and change only under stressful conditions [11]. In following, we present results focusing on values obtained for yeast cells (see also figure 2):

1. The reported cytosolic pH is approximately neutral [11]. Orij et al. [11] determined the value *7,2 ± 0,2* units in exponentially growing yeast supplied with glucose and other nutrients. In the case of starvation, *6,0 ± 0,1* units were reported. Nevertheless, cytosolic pH is not a static parameter [11]. Because presented work aims at cytosolic pH in yeast, a more detailed overview is given in section 1.2.1.

2. The value of mitochondrial pH in normally grown yeast cells is reported to be approximately *7,9 ± 0,2* and hence, it is higher than the value of cytosolic pH [11,22]. Proton gradient is thus oriented inwardly into the mitochondrion and preserved in the presence of glucose (or other energetic sources) because of ATP synthesis [23]. Only cells exposed to stressful environments (low concentration of glucose for example) have shown a reversed proton gradient between cytosol and mitochondria. Under such conditions, mitochondrial pH decreases to approximately *5,7* units [11].

3. Yeast vacuoles are reported to have an acidic pH [9,10,24,25]. Proton gradient across vacuolar membrane is subsequently used for transport of various compounds [26,27]. The actual value of vacuolar pH strongly depends on the value of extracellular pH, but remains always acidic [10].

4. The secretory pathway is described to acidify from *7,2* in the endoplasmatic reticulum to *5,2* in the secretory granules. Correct protein sorting and modification depend on well adjusted pH values inside of vesicles [28]. According to Kane, acidification correlates with biosynthesis of V-type ATPases [23.]

5. The value of pH in the peroxisomal lumen of *Saccharomyces cerevisiae* is reported to be *8,2* units. Alkaline values of pH correlate with pH optimum for most of the peroxisomal enzymes, which lies between *8* and *9* units [29].

6. Laser microspectrofluorimetry revealed that pH inside of nucleus is *0,3* eventually *0,5* units higher than in cytosol [30]. The mechanism controlling the pH gradient between cytosol and nucleus involves probably K^+/H^+ exchangers [31]. This data were obtained in higher eukaryotes (mice), no comparable data for yeast were reported to date.

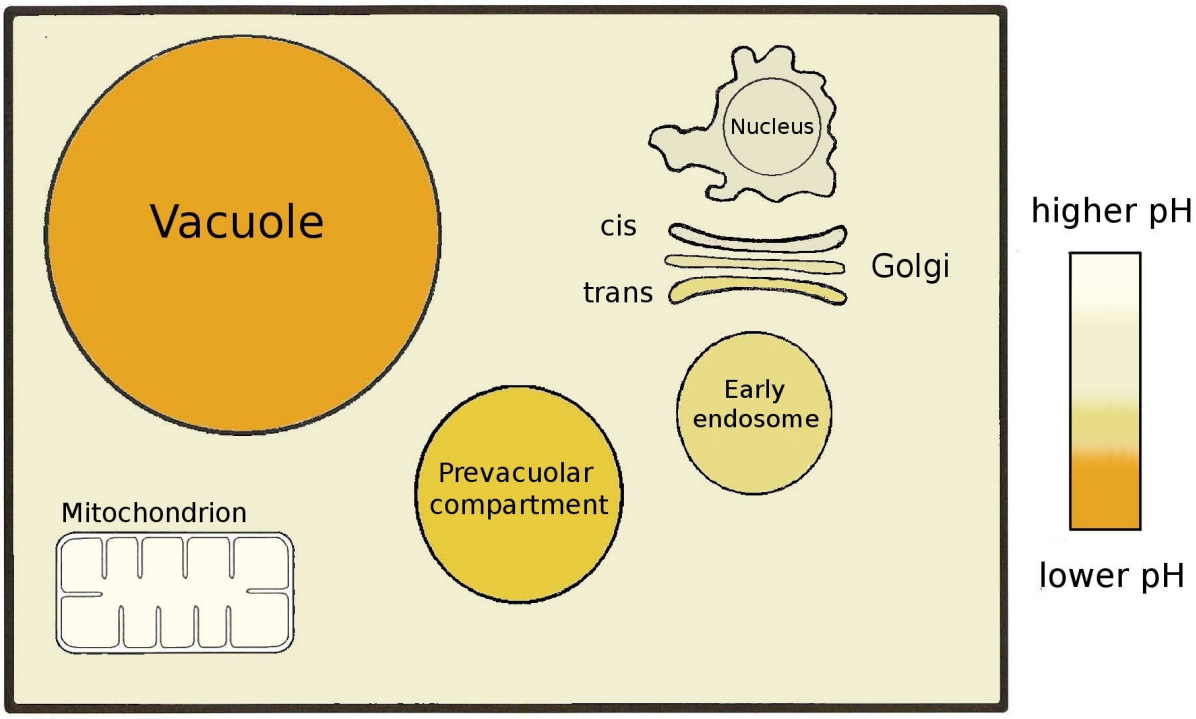

Figure 2 Schematic overview of pH homeostasis in yeast, pH in cytosol is approximately neutral and depends on selected environmental parameters.

1.2.1. Cytosolic pH in Saccharomyces cerevisiae

So far, there are no data available on pH in yeast different from *Saccharomyces cerevisiae*. Consequently, following text describes only results obtained from this one yeast species.

Experimental assays studying specifically cytosolic pH were performed by using ratiometric fluorescence protein pHluorin [9-12]. Preceding experiments using different experimental techniques were organelle-nonspecific (for details see the section 1.4.) and averaged over the whole cell structure including acidic vacuoles. Therefore, obtained results differ significantly from the actual value of cytosolic pH [11].

Cytosolic pH was determined to lie within the range of approximately *5,5* to *7,5* units. Although the range seems to be wide, only selected environmental parameters lead to deviations from the pH value of approximately *7* obtained in yeast cells exponentially growing on glucose [11]. Cytosolic pH of *7,0* is believed to be optimal for growth and yeast cell supplied with sufficient energy sources maintain it rapidly [11].

The most important factors influencing pH homeostasis of cytosol include weak organic acids [9,32], low extracellular concentration of glucose [10] and other nutrients such as galactose or glycerol/ethanol [11].

Orij et al revealed that glucose-starved yeast posses a very low cytosolic pH of approximately *6,0* units, but achieve a stable cytosolic pH of approximately *7,3* units within *30* minutes after the addition of glucose [11] (see figure 3).

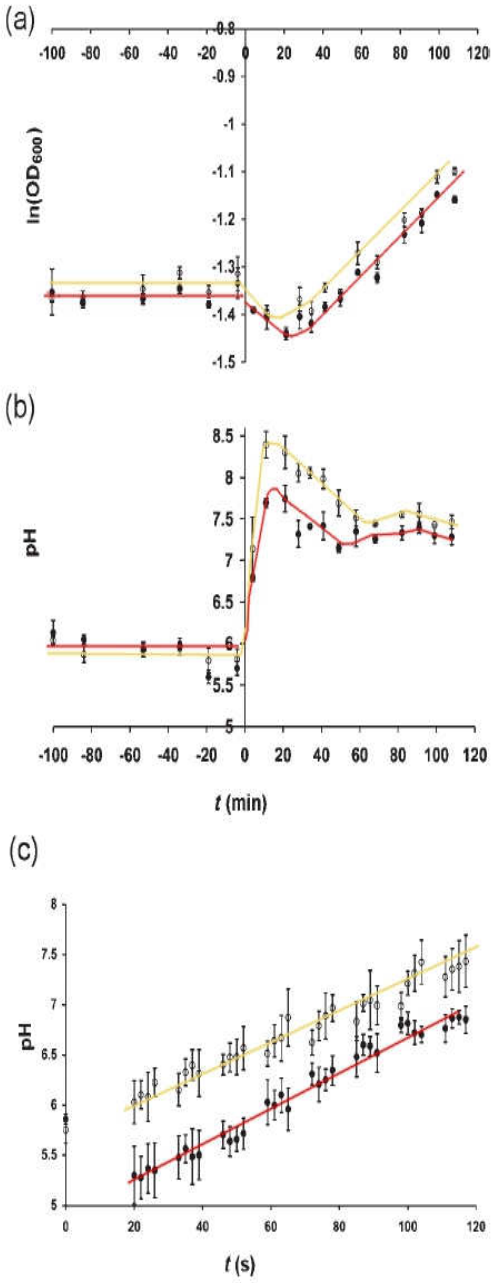

Figure 3 Time resolved glucose effect. Yellow curve represents mitochondrial pH, red stands for cytosolic pH. Glucose was added at *0 s*. Adapted from Orij et al. [11].

The same effect was previously (without time-resolved monitoring of cytosolic pH) reported by Martínez-Muñoz & Kane [10] and confirmed later by Marešová et al. [12]. Maintaining the value of pH $7{,}3 \pm 0{,}2$ seems to correlate with cell growth [11], as shown in figure 3. Similar effects were also described in relation to deprivation by other energy sources such as galactose or glycerol/ethanol [11].

Experiments monitoring both, the cytosolic and vacuolar pH, revealed also a close connection between the function of V-ATPases and cytosolic pH [10]. Mutants lacking activity of V-ATPases (known as *vma* mutants) displayed even at pH *5*, conditions optimal for the growth, significantly lower cytosolic pH than wild type yeast cells. Also, the response of *vma* mutants to glucose was smaller [10].

Only recently, Dechant et al identified cytosolic pH as a second messenger in a glucose-sensing pathway mediating the activation of the cAMP-dependent protein kinase A (PKA) pathway [21]. They identified V-ATPases as a sensor of cytosolic pH and also proposed a mechanism, how cytosolic pH acts as a signal to promote cell growth [33]. Surprisingly, Orij et al found out that environmental pH in the range of *3* to *8* units did not significantly influence the obtained values of cytosolic pH [11].

1.2.2. Transporters maintaining pH gradients inside the yeast

Lipid membranes are almost impermeable to protons and cell compartments, eventually cells as whole, are enclosed in several types of membranes. Therefore, a mechanism how to overcome such barriers has developed during the evolution. In the case of cytosolic pH, several transporters embedded within different types of membranes collaborate to achieve homeostasis as described in sections *1.2.* and *1.2.1.*

In this section, only the most important transporters involved in pH homeostasis of the whole yeast cell are discussed. Since our work aims at processes interconnected with alkali-metal and pH homeostasis, additional transporters participating in both, are described in the section 1.3. Now, we briefly summarize the most important transporters mediating proton transport in selected organelles (see also figure 5):

1. Transport of H^+ across plasma membranes of *fungi* (and also plants) is primarily maintained by P-type ATPases Pma1p [34]. According to Ambesi et al, Pma1p pumps protons out of the cells against the inwardly orientated proton gradient (energy is required) [35].

2. Respiratory chain complexes I, II, III, IV transport protons out of mitochondria into the intermembrane space and essentially contribute to the alkalinization of mitochondria. F-type ATPases usually employ the built-up proton gradient for synthesis of ATP. All of these transporters are embedded in the inner membrane of mitochondria. Complexes I, II, III and IV are directly involved in respiratory chain, whereas F-type ATPases are responsible for ATP synthesis [36].

3. Acidification of vacuoles is caused by V-type ATPases. The structure of V-type ATPases reassembles the structure of well described F-ATPases [37]. V-type ATPases are regulated by cytosolic pH (as a second messenger) [21].

4. V-type ATPases were also found in membranes of acidic organelles like lysosomes, endosome, the Golgi apparatus, secretory vesicles and clathrin-coated vesicles [38]. According to Kane, they are believed to be primarily responsible for acidification of these organelles [23].

In the following sections we give a more detailed overview of transporters described in the text above. Their role in the pH homeostasis of secretory pathway, vacuoles, mitochondria and cytosol will be described. The focus of the section will be aimed at properties influencing cytosolic pH and its interdependence with alkali metal homeostasis. For closer details we recommend reviews from Ariño et al [8], Ambesi et al. [35] and Martínez-Muñoz & Kane [39].

1.2.3. Proton pumping ATPases in the yeast membrane

Proton pumping P-type ATPases are integral proteins embedded in plasma membranes of yeasts and plants. They are encoded by genes of the *PMA* family and play crucial role in the physiology of yeast cells, where they essentially contribute to the generation of an inwardly oriented electrochemical gradient of protons across the plasma membrane. They pump protons out of cytosol into the extracellular space. The motion of protons is driven by ATP hydrolysis [40] and consumes about 20% of cellular ATP [8].

Proton pumping ATPases directly influence cytosolic pH. But according to Martínez-Muñoz & Kane, P-type ATPases have to collaborate with V-type ATPases to achieve the correct value of cytosolic pH [39]. Consequently, both are essential for maintaining pH homeostasis in cytosol.

The activity of proton pumping ATPases contributes essentially to the yeast plasma membrane potential, which is according to Nakamoto & Slayman approximately -2*00 mV* [41]. The electrochemical energy stored in proton gradient is then subsequently used for secondary transport of following compounds [42]:

1. uncharged molecules (sugars, neutral amino acids), which are transported by proton symport

2. charged molecules (anionic: chloride, phosphate, sulphate, lactate, acetate, anionic amino acids, cationic: K^+, NH^+_4, Na^+, Ca^{2+}, Mg^{2+}, cationic amino acids), which are transported by uniport or proton symport

3. undesirable compounds, which are transported by antiport

The activity of Pma1 ATPases is tightly regulated by several signals [8]. Positive regulation is rapidly achieved by addition of glucose to yeast [43]. Decreased cytosolic pH and increased potassium uptake are also reported as positive regulatory signals [44,45]. Regulation of activity induced by internal or external pH is probably connected with maintaining a relative narrow range of cytosolic pH [10]. However, molecular mechanisms controlling Pma1p are still largely unknown [8].

Pma1p is primarily responsible for building up the plasma-membrane potential in yeast. On the other hand, transport rate of Pma1p depends on conformational changes between phosphorylated states *E1-P* and *E2-P,* which are influenced by membrane potential [46]. Thus, decrease of the plasma-membrane potential positively stimulates the activity of Pma1p [47]. In 1988, Perlin et al. described the leak of protons in a yeast strain carrying a point mutation in Pma1 [48]. Since electrochemical potential present in the yeast did not explain the leak, simultaneous symport of potassium cations was proposed to occur. In other words, potassium transport and regulation of cytosolic pH seems to be interconnected (see also figure 5).

1.2.4. pH homeostasis in mitochondria

We only briefly review the importance of electron transport chain for synthesis of ATP, its connection to the presence of energy sources (glucose for example) and its coupling to the cytosolic pH. Detailed reviews are available on the topic.

Complexes *I, II, III and IV* are embedded in the inner mitochondrial membrane and are involved in electron transport chain. They are also responsible for pumping protons out of the matrix. The proton gradient is then subsequently used by F-ATPases for ATP synthesis. Figure 4 gives a schematic overview of transporters embedded in mitochondrial membrane. We want only stress out that ATP synthesis driven by F-type ATPases depends on presence of glucose or other energy sources and that an electrochemical gradient oriented inwardly into the mitochondrion is needed, consequently mitochondrial pH is reported to be higher than cytosolic pH [10].

As reported by Ariño et al, pH homeostasis of mitochondrion is coupled to the alkali metal homeostasis via (as so far known) *Mdm38* [8]. Assays performed on mitochondria isolated from *mdm38* deletion mutants revealed low membrane potential, highly reduced K^+/H^+ exchange, high potassium content in the matrix and increased volume of mitochondria. Upon the loss of its K^+/H^+ antiport function, mitochondrial swelling followed by fragmentation of mitochondrial reticulum occurred. Mitochondrial material is then subsequently digested by vacuole [49,50]. Therefore, active exchange of K^+ and H^+ is indispensable in mitochondrial physiology.

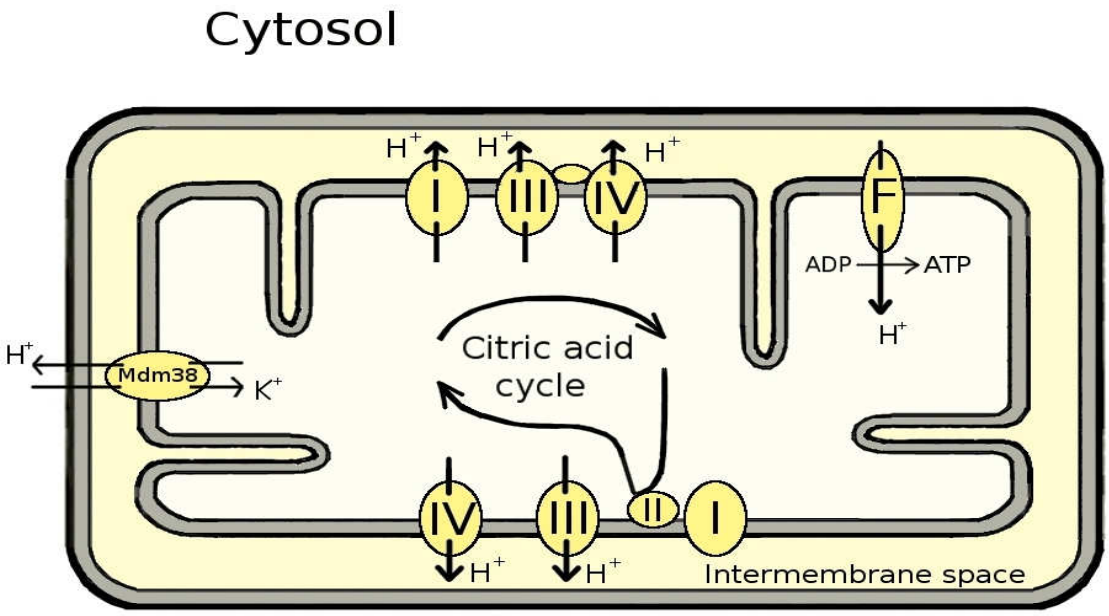

Figure 4 Selected transport systems embedded in mitochondrial membrane. Complexes I, II, III and IV are involved in electron transport chain, complex II takes part in citric acid cycle. Transport protein Mdm38 mediates K+/H+ exchange and is indispensable for proper alkali metal homeostasis in mitochondrion.

1.2.5. V-type ATPases

V-ATPases are multisubunit complexes that are present in multiple organelles. In yeast, their association with membranes of endosomes, vacuoles, Golgi-derived vesicles and clathrin coated vesicles is reported [23]. V-ATPases are indispensable for life-important cell functions:

1. Growth and pH homeostasis
2. Extrusion of waste molecules
3. Receptor mediated endocytosis
4. Protein folding, trafficking and targeting

V-type ATPases are evolutionary ancestors of F-type ATPases [51] with high degree of genetic homology reported [23]. The domain V_0 is an integral part embedded in the membrane, the domain V_1 is water-soluble and peripheral. It contains catalytic sites involved in ATP hydrolysis [51,52]. The energy released by ATP is then transferred into the domain V_0, where it is used for pumping of protons against their electrochemical gradient. V-ATPases contribute to organelle acidification and cytosolic alkalinization [53].

Domains V_0 and V_1 are reported to dissociate rapidly in the case of low glucose concentration [54]. Dissociation is reversible, after the dissociation, V_1 domains are freely available in cytosol and V_0 domains remain bound to the membranes. But proton transport does not occur [54]. Addition of glucose to yeast with dissociated V-ATPases leads to rapid reassembly of domains within minutes. Protons are then subsequently pumped into the vacuoles (and other acidic organelles) and the value of cytosolic pH rapidly increases [11]. In other words, interconnections between cytosolic pH and the functionality of V-ATPases exist.

Only recently, Dechant et al revealed that V-ATPases function also as sensors of cytosolic pH [21]. Since V-ATPases are required for full activation of the PKA pathway (as a response to the addition of glucose), they probably mediate pH signal to PKA. Since PKA pathway is conserved among higher eukaryotes, it is of high interest to elucidate the role of glucose on cytosolic pH in different eukaryotes [21].

V-ATPases consist of several structural subunits, but only subunit *a* seems to be crucial for correct targeting of V-ATPases in cell organelles. Two variants of subunit *a* were described so far [23]. The vph1p form of subunit *a* is localized to the vacuolar membranes and the isoform stv1p is cycling between the Golgi apparatus and prevacuolar compartment [55].

Different functionality and assembly ratio is crucial for explaining, how different isoforms of V-type ATPases contribute to acidification of different organelles [23]. V-ATPases are synthesized step by step. The process starts in endoplasmatic reticulum and is processing through the Golgi apparatus. Finally assemblied V-ATPases are then targeted to their final destination (regulated by *VMA12*, *VMA21* and *VMA22* genes). The ability of V-ATPases to pump protons is fully developed in their final destination, but already in Golgi apparatus proton pumping activity occurs. The activity grows in the direction of V-ATPase assembly. The growing activity of V-type ATPases explains, why the acidification of secretory pathway increases in the direction of V-type ATPase assembly [23].

1.3. Potassium and sodium homeostasis in yeast

High intracellular concentration of K^+ is essential for every living cell since K^+ is involved in a huge variety of functions including regulation of cell volume, pH homeostasis, protein synthesis and enzyme activation [56]. On the other hand, Na^+ is toxic and thus, yeast cells keep its concentration relatively low [57].

Concentration gradients of potassium and sodium are coupled to the proton gradient built up by Pma1 ATPase and are influenced by each other due to the activity of several alkali metal transporters (figure 5). It is also suggested that haloterance genes encoding proteins involved in alkali metal homeostasis takes part in regulation of cytosolic pH [57,58]. However, the molecular mechanism is still unknown [58].

Since concentration gradients of K^+ and Na^+ have an opposite direction, yeast has developed several strategies to maintain such gradients, following strategies are described [57]:

1. Higher affinity for potassium than for sodium
2. Efficient efflux of toxic cations
3. Selective compartmentation of cations in cell organelles

The general organization of transport dependent alkali-metal homeostasis in yeast conforms to the chemiosmotic model [59]. The electrochemical gradient built up by electrogenic pumps excreting H^+ or Na^+ energizes different types of transporters embedded in the plasma membrane as shown in figure 5.

The ability of yeast to maintain negatively charged, hyperpolarized state of plasma membrane [59] is essential for homeostasis of yeast. Since there are no electrophysiological measurements of yeast plasma membrane potential, only suggested values of about −200 mV are available [60,61].

On the other hand, yeast belongs to the kingdom *fungi* and extrapolations from electrophysiological measurements performed on other types of fungal cells are particularly possible. Such measurements have for example revealed that there is an relation between cytosolic pH, starvation on K^+ and membrane potential in *Neurospora crassa* [62]. Taken together with measurements of cytosolic pH (based on several fluorescence probes) in mutants lacking the activity of selected alkali metal transporters, it may suggest that alkali metal transporters form an essential part of a pathway regulating the cytosolic pH and probably the plasma membrane potential [12].

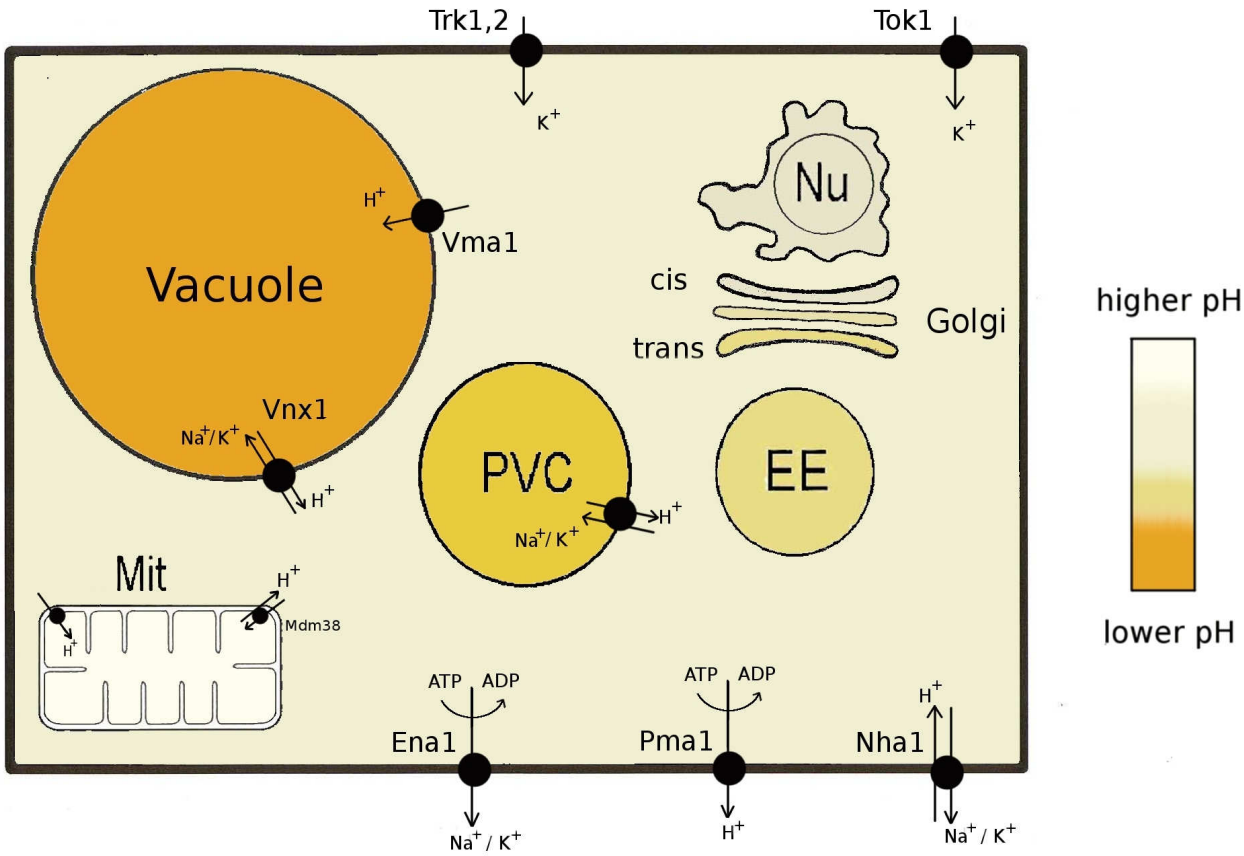

Figure 5 Major transporters involved in alkali metal and pH homeostasis embedded in the plasma membrane, in the vacuolar membrane and in the membranes of secretory pathway of *Saccharomyces cerevisiae*. Colour gradients represent a schematic overview of pH inside of yeast. Arrows indicate transport direction of the given cation. PVC is abreviation for prevacuolar compartment, EE is early endosome, Mit stands for mitochondrion and Nu means nucleus.

1.3.1. K^+ transport across the plasma membrane

The intracellular concentration of K^+ ranges from *200* to *300 mM*, whereas the extracellular concentration varies depending on environment in micro-molar range [63]. Three types of transport systems involved in K^+ uptake in yeast have been identified so far (see table 1). Generally yeast posses generally more than one K^+ uptake system [8], but none of the studied yeast species has more than two K^+ uptake systems [8]. Remarkably, only *Zygosaccharomyces rouxii* represent an exception with only one single K^+ uptake system.

The most conserved system of potassium uptake in yeast is encoded by genes of the *TRK* family, two genes *TRK1* and *TRK2* belonging to the family have been identified so far. *TRK1* seems to be conserved among yeast and only *Saccharomyces cerevisiae* and *Schizosaccharomyces pombe* are reported to posses both genes simultaneously. Interestingly, the role of *TRK2* differs significantly in both. Whereas in *Saccharomyces cerevisiae* transport activity of Trk2p is undetectable in the presence of Trk1p [8], in *Schizosaccharomyces pombe* both transporters are equally important and mutants lacking both of them are unable to grow at very low K^+ concentrations [64]. Trk1p is reported to be essential at low potassium concentrations [65,66], whereas Trk2p is described as a low affinity transporter [67]. At concentrations about 10^{-1} *M*, potassium uptake is non-specific and mediated by several types of membrane transporters [68,69].

Another potassium uptake system is encoded by the genes of *HAK* family and has been identified in many (but not in all) yeast species (see table 1). It has been proposed that Hak transporters work as K^+/H^+ symporters with a high concentrative capacity. They are expressed mostly under low external K^+ concentrations [8].

The efflux of K^+ is mediated by only one K^+ specific system known as Tok1p, which is an outward-rectifying potassium channel embedded in the yeast plasma membrane. No grow related phenotypes related to dysfunction of Tok1p have been reported so far (Ariño et al 2010) and although electro-physical properties are well known [70], physiological role of Tok1p is not understood to date [8]. Another K^+ efflux systems are Ena1p and Nha1p, which are primarily responsible for Na^+ efflux (see the following section).

Table 1 Genes encoding transporters involved in K^+ transport in yeasts. Adapted from Ariño et al. [8]. Plus sign means that selected protein is present, minus that it is not present in the given yeast species

	System for K^+ influx			K^+ channel
	TRK1	*TRK2*	*HAK1*	*TOK*
S. cerevisiae	+	+	-	+
S. pombe	+	+	+	-
D. hansenii	+	-	+	-
Z. rouxii	+	-	-	+
C. albicans	+	-	+	+
Y. lipolytica	+	-	+	+

1.3.2. Na^+ transport across the yeast plasma membrane

The Na^+ concentration is regulated by two major types of transport systems. The first system is made up of cation extrusion P-type ATPases encoded by genes of *ENA* family and is expressed at high levels [57]. Non-specific extrusion of other monovalent cations as potassium was also observed [71]. The second system is represented by Na^+/H^+ antiporters. In contrast to cation extrusion ATPases, they are expressed only at low levels [72]. The extrusion of cations uses energy stored in inwardly oriented gradient of protons [57].

Both systems cooperate to achieve alkali-metal homeostasis [57]. At alkaline extracellular pH values, mainly the Ena1 ATPase is active and at the acidic external pH, the Nha1p takes over the role of Ena1p [73]. In the absence of Ena1p alkali-metal homeostasis significantly depends on the activity of Na^+/H^+ antiporters [57].

Na^+ efflux system belonging to the *ENA* family was shown to form a cluster. In the case of *Saccharomyces cerevisiae*, various non-identical copies of *ENA* gene have been identified [8]. The *ENA1* gene has been identified also in the yeast of *Zygosaccharomyces rouxii* [74]. *ENA1* is reported to be primarily responsible for sodium tolerance in Saccharomyces cerevisiae [8]. Deletion mutants possessing none of the Ena transporters were strongly sensitive to sodium

and lithium cations [75-77], they displayed also a significant growth defect at high pH values [75]. Nevertheless, only the expression of one single gene from the *ENA* cluster, namely *Ena1*, restored the salt tolerance. Expression of Ena1p from *Saccharomyces cerevisiae* in other fungi [78] revealed its ability to increase Na^+ and Li^+ tolerance. A decrease of intracellular Na^+ and Li^+ content was also observed [8].

The second transport system is made of Na^+/H^+ antiporters. In the case of *Saccharomyces cerevisiae*, it is encoded by genes belonging to the *NHA* family. Based on Hill equation of enzyme kinetics, Tse et al. determined that one Na^+ cation and two binding sites for H^+ allosterically influence each other [79]. Non-specific Li^+ and Rb^+ transport mediated by *Nha1* was also observed [57,73]. Properties of Nha1p are more closely discussed in following sections. Now, we only want to stress out that Nha1p is also involved in pH homeostasis of yeast [57].

Table 2 Genes encoding transporters involved in Na^+ transport in yeasts. Adapted from Ariño et al (2010). Plus sign means that selected protein is present, minus that it is not present in the given yeast species. Question marks means the lack of data.

	Na^+/H^+ antiporters		Na^+ efflux
	NHA	*SOD2*	*ENA1*
S. cerevisiae	+	?	+
S. pombe	?	+	?
D. hansenii	?	?	?
Z. rouxii	+	+	+
C. albicans	+	?	?
Y. lipolytica	+	?	?

1.3.3. Na^+/H^+ antiporters in yeast

Na^+/H^+ antiporters form a large family of transporters present in most eukaryotes. They are embedded in plasma-membrane and also in organelle-membranes, where they are responsible for detoxification from surplus sodium cations, the maintenance of pH and potassium homeostasis [7]. According to Pribylová et al. and Bañuelos et al., the family of yeast plasma membrane Na^+/H^+ antiporters can be divided in two distinct subfamilies [7,80]:

1. Antiporters with substrate specificity only for Na^+ and Li^+ responsible for primary detoxification of cells

2. Subfamily of antiporters mediating transport of at least four alkali metal cations responsible for regulation of intracellular K^+ concentration, pH and cell volume. They also play a role in elimination of toxic cations.

So far, Na^+/H^+ antiporters were identified in several yeast species. They are known as Nha1p in *Saccharomyces cerevisiae* [81] and *Debaryomyces hansenii* [82], as Cnh1p in *Candida albicans* [83], as ZrNha1p and ZrSod2p in *Zygosaccharomyces rouxii* [74,83], as YlNha1p (eventually as YlNha2p) in *Yarrowia lipolytica* and as Sod2p (eventually Sod22p) in *Schizosaccharomyces pombe* [8].

In the case of *Saccharomyces cerevisiae,* it was shown that *nha1* deletion mutants display an increased cytoplasmatic pH and display different behaviour in presence of K^+. Thus, the addition of KCl to starved *nha1* deletion mutants caused higher alkalinization of cytoplasmatic pH compared to the wild type cells [84].

Remarkably, yeast species closely related to *Saccharomyces cerevisiae* encode usually only one Na^+/H^+ antiporter which posses broad substrate specificity for at least four cations [7,82,85]. Evolutionary more distant species (*Yarrowia lipolytica* and *Schizosaccharomyces pombe*) posses two proteins belonging to the Na^+/H^+ antiporter family. One of them is involved in detoxification and the second one takes part in pH and potassium homeostasis [86-88].

1.3.4. Na^+/H^+ antiporters in S. cerevisiae and Z. rouxii

Saccharomyces cerevisiae posses only one Na^+/K^+ antiporter with a broad specificity for different cations. On the other hand, the 732^T strain of *Zygosaccharomyces rouxii* was reported to posses two Na^+/H^+ antiporters. They were named ZrNha1p and ZrSod2-22p [7]. In a different strain of *Zygosaccharomyces rouxii* (the ATCC 42981 strain) two other genes were identified. They are known as *Z-Sod2* [74] and *Z-Sod22* [89]. However, ZrSod2–22p display *99.7%* identity with Z-Sod2p and *83.9%* identity with *Z-Sod22* [83]. As a consequence, all three genes are believed to be allelic. None of the encoded proteins transports K^+ and ZrSod2–22p was confirmed to transport only Na^+ and Li^+ [8]. Both *Z-Sod2p* and *Z-Sod22p* enhance the NaCl tolerance of a salt-sensitive *Saccharomyces cerevisiae* strain, but only *Z-Sod2* was confirmed to be transcribed in *Zygosaccharomyces rouxii* cells [74,89].

Sequence analysis performed by Pribylová et al. clearly demonstrated that ZrNha1p and ScNha1p are more closely related to each other than ZrSod22p and ScNha1p eventually ZrNha1p and ZrSod2-22p [7]. In other words, primary and secondary structure of ZrNha1p resembles the structure of ScNha1p. Genetic and structural homology causes also similar transport properties as described by Pribylová et al. [7]. It was shown that ZrNha1p posses affinity for both K^+ and Na^+ cations and consequently seems to express similar broad affinity for different cations as the ScNha1p. However, ZrNha1p seems to prefer K^+ to Na^+ [7].

The contribution of Na^+/K^+ antiporters to the salt tolerance has been studied in two ways: by expressing the genes from a plasmid in a *Saccharomyces cerevisiae* mutant strain lacking both Na^+-ATPase and Na^+/H^+ antiporter genes (*ena1-4*Δ *nha1*Δ) [7] and also by studying them in their native surrounding [7,12]. The impact of Na^+/K^+ antiporters on pH homeostasis was studied exclusively in *Saccharomyces cerevisiae* [12], so there are no data available for *Zygosaccharomyces rouxii.*

The expression of ZrSod2-22p from *Zygosaccharomyces rouxii* in *ena1-4* and *nha1* deletion mutants revealed its high transport capacity for lithium and sodium, but K^+ and Rb^+ were not recognized as substrates. The Nha1p from *Saccharomyces cerevisiae* displayed a broad substrate specificity for at least four alkali metal cations [13], but the contribution to the overall cell tolerance at high external concentration of Na^+ or Li^+ cations seemed to be lower than in the case of Na^+/K^+ antiporters from *Zygosaccharomyces rouxii* [13,14].

1.4. Measurements of pH in yeast

Due to high mobility and rather small dimensions of yeast cells, microelectrodes are inappropriate for measurements of pH in living yeast [12]. From this reason several different experimental techniques have been developed:

1. In 1950 Conway and Downey performed measurements using microelectrodes. To enable the measurements an invasive procedure was performed (yeast was frozen and then rapidly thawed up) [90].

2. Equilibrium distribution of radioactively labelled weak acids or bases in the yeast cells revealed intracellular pH indirectly [90].

3. To quantify intracellular pH the amount of benzoic acid inside the biomass and in the supernatant was measured [91].

4. Dynamic intracellular pH measurements were performed by applying low concentration pulse of benzoic acid to the yeast cells [92].

5. Nuclear magnetic resonance of ^{31}P is a non-invasive technique to monitor intracellular pH changes in time scales of about 100 seconds [93,94,94].

6. Cells were loaded with several pH-sensitive fluorescence probes, whereby pH could be monitored continuously [95-97].

7. Inducing production of fluorescence protein probes by inserting plasmids carrying genes encoding them enables continuous pH measurements [9,12,98,99].

In this work we have measured cytosolic pH of yeast using the fluorescence probe pHluorin. Since pHluorin is a pH sensitive derivative of Green Fluorescence Protein the following sections review the most important facts about GFP and pHluorin. The focus is aimed at properties influenced by pH.

1.4.1. Green fluorescent protein

Shortly after the discovery of Green Fluorescent Protein (GFP), excitation and emission spectra of GFP were obtained [100]. It was shown that excitation spectrum of GFP is bimodal and peaks at *395* and *475 nm* (figure 6). However, the intensity of fluorescence at *475 nm* is very low. The emission spectrum peaks only at *508* nm. Consequently, GFP converts blue excitation light into green fluorescence light, just as the name of *GFP* suggests.

Fluorescence properties of GFP are tightly connected to reactions influencing protonation states of GFP. No essential conformational changes between pH values *5,5* and *10* imply that protonation–deprotonation reactions are constrained. According to Miesenbock et al., protonation involves only the amino acid residue *Tyr66* [99]. Only two protonation states were identified [99,101]:

1. neutral form of the chromophore excitable at *395 nm*
2. ionized form, excitable at *475 nm*.

Prasher et al. [102], Chalfie et al.[103] and Inouye & Tsuji [104] expressed GFP in several organisms to demonstrate its abilities as a fluorescence probe. Generally, fluorescence probes derived from GFP can be classified in two families: ratiometric (for example pHluorin) or nonratiometric (for example EGFP). To date EGFP has been used to monitor cytosolic pH in Golgi apparatus [105] and in synaptic vesicle cycling at nerve terminals [106]. For measuring pH especially in organelles of yeast, ratiometric methods are better suitable. In yeast, ratiometric GFPs were used to measure cytosolic pH [9,11,12,39] and mitochondrial pH [11].

1.4.2. GFP derivative pHluorin

Using the structure-directed combinatorial mutagenesis Miesenbock et al. prepared a modified version of GFP called pHluorin [99]. The modified version increased the gain of fluorescence in its deprotonated state (figure 6). Thus, only the ratio of fluorescence at two distinct wave lengths has to be monitored. Intracellular concentration of pHluorin therefore does not interfere with measurements of intracellular pH. Since conformational changes of pHluorin follow pH changes instantly, pHluorin is suitable for measurement of pH in real time [11,12,99].

Insertion of plasmids encoding pHluorin employs the cell apparatus itself to synthesize the fluorescent probe and no additional staining procedures are required [12]. Proper signal sequences enable us to control the targeting of pHluorin in selected cell organelles [107]. As reported by Orij et al., the expression of pHluorin in yeast has no significant impact on their physiology [11] and pHluorin therefore represent an easy to handle, non-invasive and organelle-specific method of pH measurement. Studies using pHluorin were performed in several strains of *Saccharomyces cerevisiae* [9,11,12,29,39]. To our knowledge, there are no data about intracellular pH in other yeast species (such as *Zygosaccharomyces rouxii*) available to date.

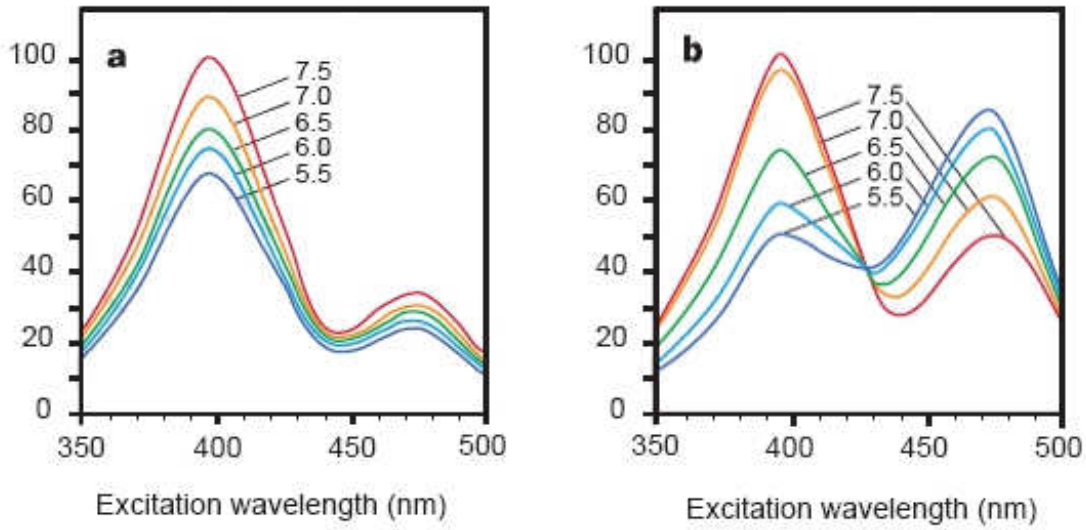

Figure 6 Excitation spectra of a wild-type GFP (a) and its ratiometric derivative pHluorin (b). Spectra were obtained *in vitro* by Miesenbock et al [99]. Samples contained 27.5mM chromophore, 50mM sodium cacodylate, 50mM sodium acetate and were adjusted to the indicated pH values. The ordinate scales reflect normalized differences in emitted fluorescence intensity. Adapted from Miesenbock et al [99].

1.4.3. Buffering capacity of yeast

As shown in sections *1.2.* and *1.2.1.*, under constant environmental conditions yeast maintain cytosolic pH in a relatively narrow range. In other words, cytosol behaves similar as a chemical buffer and buffering capacity is used to describe its properties. We define it in the following way: buffering capacity β equals the amount of strong base (eventually strong acid), that increases (decreases) the cytosolic pH by one unit:

$$\beta = \frac{\Delta B}{\Delta pH}$$

In chemical buffers only purely physico-chemical processes are involved in maintaining a relatively narrow range of pH as a response to addition or removal of H^+ from the solution. But in yeast, there are two additional mechanisms involved: active transport of protons across the plasma or organelle-specific membranes and metabolic pathways. Since transport mechanisms respond faster than metabolic pathways, the relative contribution of both can be separated by time-resolved measurements.

In this approach, the extracellular space is rapidly alkalinized by addition of a weak base *B* (such as ammonium chloride) to a defined concentration $[B]_{total}$. The extracellular space contains dissociated and electrically neutral molecules of weak base B. Neutral forms can cross the plasma membrane of yeast by a simple diffusion and increased cytosolic pH can be observed. In the equilibrium state a steady concentration of dissociated base *B* can be calculated, we label the concentration of dissociated base *B i*n the cytosol as $[BH]_{int}$. The buffering capacity can be then expressed as follows:

$$\beta = \frac{[BH^+]_{\text{int}}}{\Delta pH}$$

where ΔpH_{int} labels the change of cytosolic pH and the concentration of dissociated molecules of weak base has to be computed from the following equation:

$$[BH^+]_{\text{int}} = \frac{[B]_{total}\ [H^+]_{\text{int}}}{(K_a + [H^+]_{ext})}$$

where K_a is the dissociation constant of NH_3, $[H^+]_{ext}$ is the proton concentration in the buffer and $[H^+]_{int}$ is the intracellular proton concentration after the increase of cytosolic pH.

The buffering capacity of cell-free extract from yeast was studied by two groups [108,109], but no influence of biological processes on buffering capacity could be determined due to the experimental techniques used. Marešová et al. measured the buffering capacity *in vivo* by quantifying the effects of addition of ammonium chloride to citrate-phosphate buffers and buffering capacity of approximately $50 \pm 15\ mM$ was determined [12].

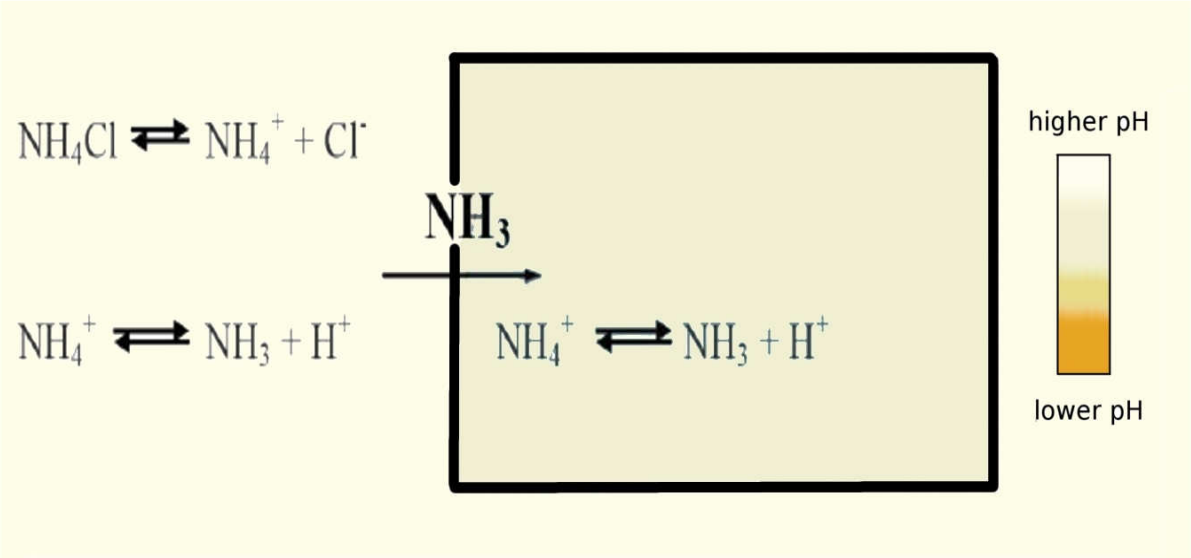

Figure 7 Schematic overview of measurements determining buffering capacity of cytosol. For sake of clarity ammonium chloride was selected as a weak base.

2. Methods

2.1. Yeast strains and transformation plasmids

Measurements of cytosolic pH were performed in two yeast species: in *Saccharomyces cerevisiae* (yeast strains BY4741 and BY4742) and *Zygosaccharomyces rouxii* (yeast strain CBS 732^T). Selected yeast strains possessed all an *ura3* mutation (see table 3). To assess the influence of selected alkali-metal transporters on cytosolic pH, mutants with affected sodium transport were constructed. Mutant strains with deleted genes *nha1*, *ZrNha1* or *ZrSod2-22* have the corresponding genes replaced either with the *kanMX* or l*oxP* cassette (see table 4).

To determine cytosolic pH transformation using plasmids pHl-U (known also as pVT100U) and pHl-G was performed. Beside of the gene for pHluorin synthesis, both plasmids contain selection markers. In the case of pHl-U, the gene *URA3* enables uracil synthesis and thus allows the selection of transformed yeast by using growth media without uracil.

The pHl-G plasmid was constructed from pHl-U by replacing *URA3* with the *kanMX* cassette. By subsequent genetic manipulations, genes required for geneticin resistance were added (for details see Marešová et al. [12]). Thus, yeast transformed by pHl-G was resistant against geneticin, but supply of uracil was required.

Table 3 Designation of yeast strains used in this work. Yeast strains used in this wotk were not able to synthesize uracil without additional genetic manipulation.

	Yeast species	**genotype**
BY4741	Saccharomyces cerevisiae	MATa his3 leu3 met15 ura3
BY4742	Saccharomyces cerevisiae	MATα his3 leu2 lys2 ura3
CBS 732^T	Zygosaccharomyces rouxii	ura3

Table 4 Selected haloterance genes from yeast strains of *Saccharomyces cerevisiae* and *Zygosaccharomyces rouxii* were deleted. In the table an overview is given of the whole genotype and designations used in this work.

	Yeast strain	**Genotype description**	**deleted transporter**
Sc1 WT	BY4741	MATα his3 leu3 met15 ura3	*none*
Sc2 WT	BY4742	MATα his3 leu2 lys2 ura3	*none*
Sc2 Nha1Δ	BY4742	MATα his3 leu2 lys2 ura3 *nha1Δ::kanMX*	*nha1p*
Zr WT	CBS 732^T	ura3	*none*
Zr Nha1Δ	CBS 732^T	ura3 nha1*Δ*::loxP	*ZrNha1p*
Zr Sod2-22Δ	CBS 732^T	ura3 sod2-22*Δ*::loxP	*Zr Sod2-22p*
Zr Nha1Δ Sod2-22Δ	CBS 732^T	ura3 sod2-22*Δ* nha1*Δ*::loxP	*ZrSod2-22 p ZrNha1p*

2.1.1. Growth media

Mutant strains transformed by pHl-U were grown in the minimal medium YNB without uracil. Mutants transformed by pHl-G were grown either in the full medium YPD containing geneticin at 1mg/ml concentration or in YNB medium containing uracil at 76 mg/l concentration and geneticin at 1mg/ml concentration. Storage was performed at approximately *4ºC*.

Table 5 Composition of YPD (YEPD) - the full medium. Agar was added for cultivation and storage of yeast in Petri plates, liquid form of YPD was prepared without agar. Glucose was autoclaved separately from yeast extract and bactopeptone.

compound	**concentration**	**amount**
bactopeptone	2 %	20 g/l
yeast extract	1 %	10 g/l
glucose	2 %	20 g/l
agar*	2 %	20 g/l

Table 6 Composition of YNB - the minimal medium. Agar was added for cultivation in Petri plates. Glucose was autoclaved separately YNB and the supplement URA were filtered (MILLEX® GP, Millipore Express, 0,22 μm filter) and mixed together at room temperature. Geneticin and uracil were used only for cultivation with selection on geneticin.

compound	**concentration**	**amount**
YNB	0,17 %	1,7 g/l
URA	0,19%	1,92 g/l
glucose	2 %	20 g/l
agar*	2 %	20 g/l
uracil*	0,08%	76 mg/l
geneticin*	1,00%	1 g/l

2.1.2. Cultivation of S. cerevisiae and Z. rouxii

Yeast was cultivated in Erlenmayer flasks (volume of *50* eventually *100 ml*) in fluid growth media described in previous section. During the growth, flasks were shaken and the temperature was kept stable at *30ºC*.

Yeast prepared for measurements of cytosolic pH were cultivated in two steps. In the first step, cells were grown into the stationary phase, then a specified amount of yeast (optical density *0*,2) was transferred into the same type of growth medium and yeast was grown into the mid-exponential phase. The two step cultivation helps to synchronize the yeast for pH measurements.

Growth curves of *Saccharomyces cerevisiae* were previously obtained by Marešová et al under the same conditions as employed in this work [12]. According to the obtained growth curves, *Saccharomyces cerevisiae* strains reached the mid-exponential phase after approximately *6* hours of growth in YNB and the stationary phase after *16* hours.

Growth curves for *Zygosaccharomyces rouxii* were obtained for all strains described in table *4* (see figure 8). All *Zygosaccharomyces rouxii* strains were transformed by pHl-U plasmid. Therefore, YNB without uracil was used as growth medium. Growth curves were obtained by transferring a specified amount of yeast (grown into stationary phase) into a fresh YNB

medium (initial optical density of *0,2* units). *Zr WT* reached the mid-exponential phase after *18* hours, *Zr Nha1Δ* and *Zr Sod2-22Δ* after *24* hours. *Zr Nha1Δ Sod2-22Δ* reached the mid-exponential phase after *27* hours of growth. After *48* hours of growth all four strains reached the stationary phase.

Optical density was measured at *578 nm* in polymethylmethacrylate cuvettes with 3ml volume. Two different instruments Novaspec II and Novaspec III were used. Although optical density is well defined physical quantity, values obtained by Novaspec III did not match exactly the values defined by Novaspec II, so a conversion formula was used and only values defined by Novaspec II are given in this work.

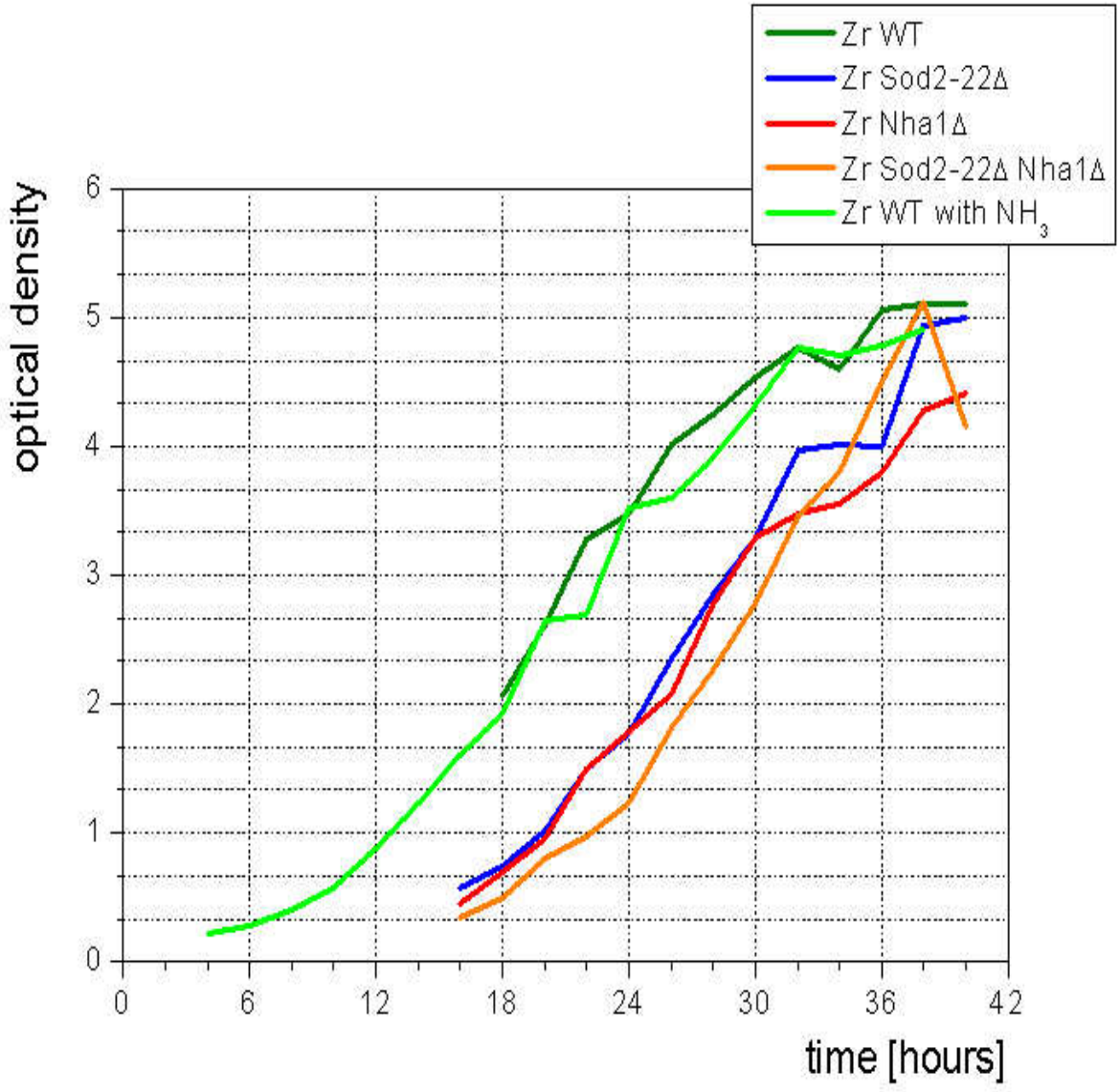

Figure 8 Growth curve obtained for *Zr WT* and three deletion mutants. *Zr WT* reaches the mid-exponential phase after approximately *18* hours, *Zr Nha1Δ* and *Zr Sod2-22Δ* after *24* hours. *Zr Nha1Δ Sod2-22Δ* reached the mid-exponential phase after *27* hours of growth. After *48* hours of growth all four strains reached the stationary phase.

2.2. Fluorescence measurements

To determine cytosolic pH in *Saccharomyces cerevisiae* and *Zygosaccharomyces rouxii*, the ratiometric fluorescence probe pHluorin was used. Its fluorescence signal was measured on FluoroMAX-II spectrophotometer (Jobin-Yvon Spex) by applying emission wavelength of *520 nm*. Fluorescence was monitored at a right-angle to the incident beam. Samples were measured in polymethylmethacrylate cuvettes (*3 ml* volume, optical density of *0,2* units).

Excitation spectra (emission wavelength at *520 nm)* were integrated over *0,4* seconds with excitation and emission slits of monochromators set at *5* nm. Measurements of cytosolic pH required to measure fluorescence signal only at excitation wavelengths of *410* and *470 nm* (emission wavelength of *520 nm)*. The obtained values were then divided and the fluorescence ratio $I_{410/470}$ was calculated. Excitation and emission slits of monochromators were set at *3 nm*, integration time at *1* second.

Preparation of samples containing living yeast required to separate yeast from growth medium (YNB and YPD give rise to a significant fluorescence signal). Mid-exponentially growing yeast was therefore harvested by centrifugation and washed twice in distilled water. A suspension of washed yeast in distilled water was prepared. Finally yeast suspension was added to a selected type of buffer (to a final optical density of *0,2* units). The centrifugation procedure required about *25* minutes. During this time no energy sources were available to yeast.

2.2.1. Calibration Buffers

Excitation spectra of pHluorin obtained *in vitro* and *in vivo* are influenced by different surroundings [22,99]. Therefore, fluorescence of pHluorin has to be calibrated *in vitro*. Calibration requires manipulation of cytosolic pH to a desired and quantifiable value. Thus, buffers titrated to desired values are prepared to contain compounds which either enable movement of proton across the plasma membrane, or compounds which disable yeasts mechanisms of controlling cytosolic pH (we discuss the problematic more closely in section 3.1.5.). After a properly selected time of incubation an equilibrium state is reached, in which cytosolic and extracellular pH are believed to be the same.

In this work, calibration was performed by using buffers titrated to six different but specified values of pH**.** The composition of calibration buffers (see table 7) matches exactly the parameters employed by Marešová et al [12]. Table 7 does not list ionophores (as used by Brett et al [9] and Martínez-Muñoz & Kane [39] since they were shown (see section 3.1.5.) to have a negligible impact on calibration. Calibration buffers were titrated to the desired pH values by adding NaOH eventually HCl.

Table 7 Composition of one litre of calibration buffer, ionophores are not listed.

Compound	Concentration	Mass
MES	50 mM	10,66 g/l
HEPES	50 mM	11,9 g/l
Ammonium acetate	200 mM	15,4 g/l
KCl	50 mM	3,73 g/l
NaCl	50 mM	2,92 g/l
2-deoxy-D-glucose	10 mM	1,64 g/l
Sodium azide	10 mM	0,65 g/l

2.2.2. Measurements of cytosolic pH and buffering capacity

To obtain cytosolic pH and buffering capacity under controlled conditions, two types of citrate-phosphate buffers (CP buffers) were prepared. The potassium buffer was prepared by dissolving *30 mM* K_2HPO_4 in one litre of distilled water. Similarly, sodium CP buffer was prepared by dissolving *30mM* Na_2HPO_4 in one litre of distilled water. CP buffers were titrated with citric acid to either pH 6 or pH 8.

To determine buffering capacity yeast was incubated in citrate-phosphate buffers at pH 8 (incubation time of *10* minutes for *Saccharomyces cerevisiae* and *15* minutes for *Zygosaccharomyces rouxii*). Ammonium chloride was then added to the final concentration of *10 mM*, samples were stirred and the fluorescence ratio was monitored through the whole procedure. The initial value (value before adding ammonium chloride) and final value (after the addition of ammonium chloride) were recorded and buffering capacity was calculated according to the formulae in section 1.4.3.

2.3. List of chemical compounds

Table 8 lists the compounds used in this work. Details about manufacturer and purity of the compounds are described.

Table 8 List of compounds used in this work

Compound	Description
2-deoxy-D-glucose	2- Deoxy-D-glucose, Grade II, min 98 %, SIGMA eventually 2 -Deoxy -D -glucose, FLUKA
agar	ROTH
ammonium acetate	ammonium acetate SigmaUltra, minimum ≥ 98%, SIGMA
ammonium chloride	SIGMA
bactopeptone	OXOID LP0037, total nitrogen 14,0
citric acid	citric acid, PENTA
geneticin	G418, disulphate salt, SIGMA
glucose	D-glucose, PENTA
HCl	SIGMA
HEPES	HEPES ≥ 99,5 %, SIGMA
KCl	SIGMA
MES	MES, low moisture content, SIGMA
NaCl	Fluka, minimum ≥ 99,5%
NaOH	SIGMA
sodium azide	Sodium azide, SigmaUltra, SIGMA
URA	Yeast Synthetic Drop – out Medium Supplement Without Uracil, SIGMA
yeast extract	Yeast Extract SERVABACTER
YNB	Difco, Yeast nitrogen base w/o Amino Acids

3. Results

3.1. Calibration

Because excitation spectra obtained *in vitro* and *in vivo* are influenced by different surroundings [22,99], calibration of fluorescence ratios obtained in living yeast is necessary. In this way, calibration points are obtained, which were then fitted with sigmoidal curve according to section 3.1.3.

In section 3.1.1, we show that calibration medium itself has a significant fluorescence signal at *410 nm*. To suppress its impact on calibration, we have employed a correction (see section 3.1.1.). In section 3.1.2., we demonstrate that correction is crucial for proper calibration. Otherwise (without correction) systematic error of about *0,6* units of pH can occur. Calibration curves for strains used in this work are presented in the section 3.1.3. and the following section discusses the role of properly adjusted incubation time on calibration. In section 3.1.5., we demonstrate that ionophores do not influence the obtained calibration curves and thus can be omitted.

3.1.1. Correction to the background fluorescence of calibration buffers

Excitation spectra (emission wavelength *520 nm*) of pure calibration buffers revealed a relative high fluorescence signal (see figure 9). To asses the impact of different pH values of calibration buffers on the signal acquired, we have used buffers titrated to six different values in the range of *5,5* to *8,0* units, but no significant differences were observed. The obtained excitation spectra at different values of pH were then averaged. The resulting background signal was then plotted against excitation wavelengths and compared with fluorescence signal from pHluorin (see figure 9). The comparison revealed that both are comparable and correction to the background signal is necessary (see the text below).

To quantify which compounds contribute to the background signal the most, we have dissolved the constituents of calibration buffer in distilled water. KCl, NaCl and sodium azide were dissolved together (referred as mixture of salts). MES, HEPES, 2-Deoxy-D-glucose and ammonium acetate were dissolved separately. The obtained spectra are presented in figure 10

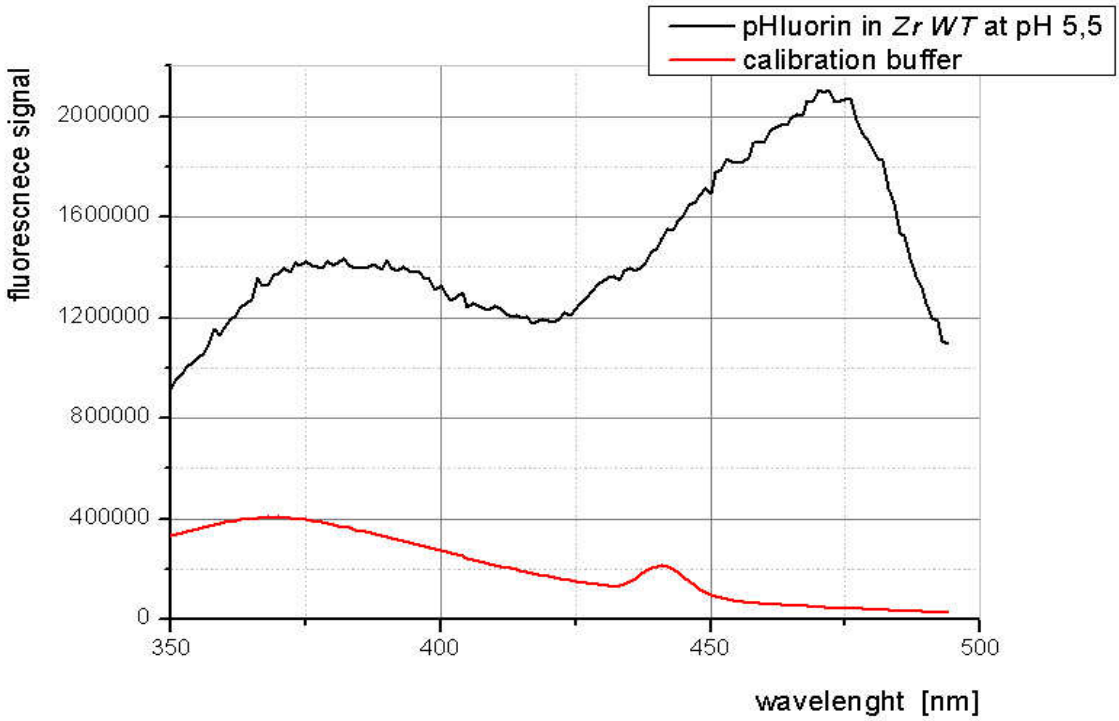

Figure 9 Excitation spectra of water, calibration medium (averaged over pH values) and pHluorin obtained from *Zr WT* (in typical concentration as used for measurement of cytosolic pH). Emission wavelength was set *520 nm.* At *410 nm* the fluorescence signals from calibration buffer and pHluorin are comparable. At approximately *440 nm* Raman peak of water is visible.

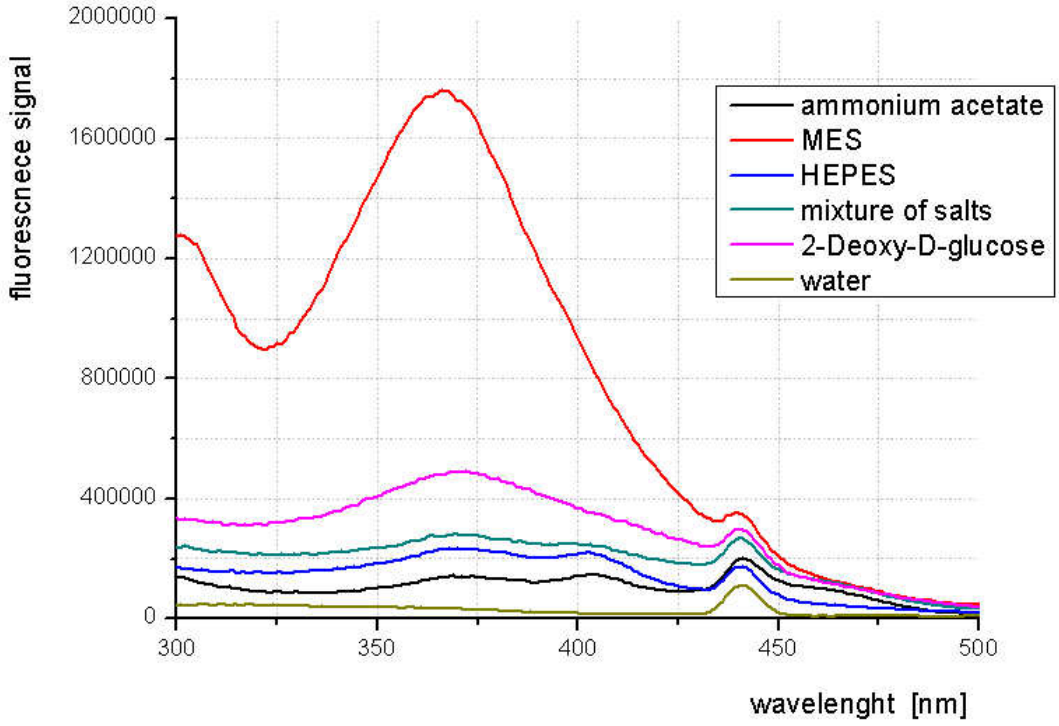

Figure 10 Excitation spectra of compounds contained within calibration buffer. Compounds were dissolved in distilled water at five times greater concentration compared to the concentrations used in calibration buffer. At approximately *440 nm* Raman peak of water is visible.

Excitation spectra for calibration buffer and pHluorin in living yeast were acquired under the same conditions (described in section 2.2.). Therefore, excitation spectra of pHluorin in living yeast (sections 3.2. and 3.3.) can be corrected directly by subtracting the spectrum of calibration buffer from the spectrum of pHluorin.

In the case of cytosolic pH measurements a different approach has to be used. The actual measurements of cytosolic pH were performed in citrate-phosphate buffers, but calibration curves are acquired from calibration buffers. Thus, only the difference between background signal from calibration buffer and citrate-phosphate buffer has to be subtracted. The background signal of citrate-phosphate buffers was proofed to be independent from the amount of sodium or potassium salts used.

By comparison of signal acquired from calibration and citrate-phosphate buffer (under conditions applied during measurements of cytosolic pH), we were able to quantify the differences (see table 9). Correction procedure involved the subtraction of 58000 units from signals acquired at *410 nm and 2000* units at *470 nm* (fluorescence in arbitrary units).

Table 9 Values of signals obtained form different buffers under conditions used for measurements of cytosolic pH.

	signal at *410 nm*	signal at *470 nm*
calibration buffer	68000	7000
citrate-phosphate buffer	10000	5000

3.1.2. The impact of correction on measurement of cytosolic pH

In this section, we demonstrate the impact of correction on correct measurement of cytosolic pH. Calibration points were obtained from living yeast after *10* (*Saccharomyces cerevisiae*) eventually *15* minutes (*Zygosaccharomyces rouxii)* of incubation in calibration buffer (see section 3.1.4. for settings of incubation times).

To demonstrate that significance of correction grows with decreasing fluorescence signal obtained from living yeast, two cases are presented. As the case of low fluorescence signal, the strain *Sc2 WT* transformed by pHl-G plasmid is presented. The strain *Sc2 WT* transformed by pHl-U plasmid is used to present the case of relatively high fluorescence signal. Corrected and uncorrected calibration curves for both are shown in figure 11.

Generally, corrected calibration curves lie under the uncorrected curves (see figure 11). Correction is performed to reduce only the fluorescence signal from compounds present in calibration buffers (the background signal from water remains) and thus, fluorescence ratios obtained in citrate-phosphate buffers do not require any correction.

Subsequently, by using uncorrected calibration curves lying below the corrected curves we would obtain lower values of cytosolic pH. In the case of *Sc2 WT* transformed by pHl-G, the fluorescence ratio of *1,0* returns cytosolic pH of approximately *6,2* units by using the uncorrected calibration curve and approximately *6,8* by using corrected calibration curve. Thus, using uncorrected calibration results in a systematic error of approximately *0,6* units. In the case of *Sc2 WT* transformed by pHl-U, the correction is much lower, only about *0,2* units. Taken together, the higher is the fluorescence signal, the less important is the correction.

Correction to the background fluorescence in *Sc2 WT* also revealed that error bars increase significantly after the correction. This effect occurs due to relative high intensity of noise when compared to the low fluorescence signal obtained from *Sc2 WT* transformed by pHl-G. The increase of uncertainty for other strains used in this work was less significant because of lower signal-to-noise ratio.

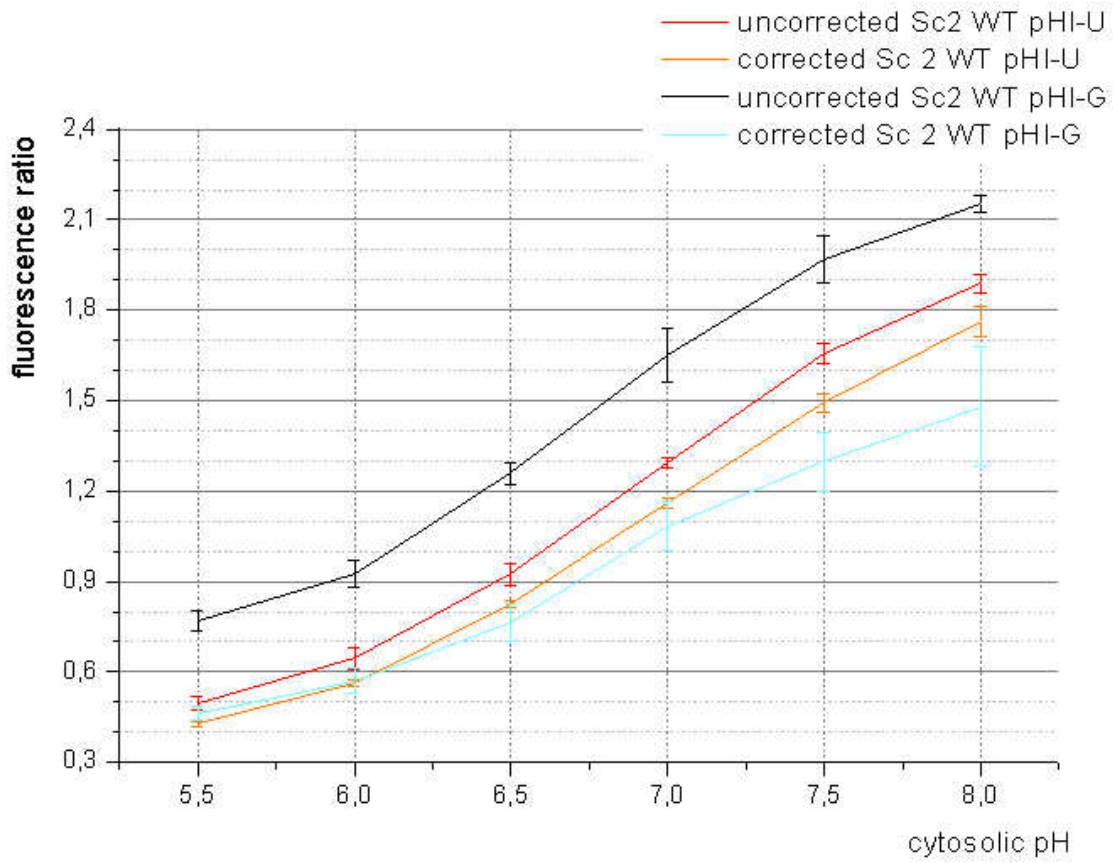

Figure 11 Comparison between uncorrected and corrected calibration curves for strain *Sc2 WT* transformed by pHl-G (red and wine) and for *Sc2 WT* transformed by pHl-U. At fluorescence ratio *1,0* uncorrected curve for transformation with pHl-G returns cytosolic pH of approximately *6,2* units, whereas corrected curves gives a value of approximately *6,8* units. In the case of yeast transformed by pHl-U, only a correction of approximately *0,2* units is observable.

3.1.3. Corrected calibration curves and their reproducibility

Calibration points were obtained from living yeast after *10* (*Saccharomyces cerevisiae*) eventually *15* minutes (*Zygosaccharomyces rouxii)* of incubation in calibration buffers of specified pH. Calibration buffers according to table 7 were used (no ionophores were added). Incubation times were selected in accordance to section 3.1.4. Calibration points (after the correction) for every yeast strain used in this work are presented in table 10 for *Saccharomyces cerevisiae* and in table 11 for *Zygosaccharomyces rouxii*. The fluorescence ratio $R_{410/470}$ was measured in several biological replicates of the given strain (see tables 10 and 11), then subsequently averaged and plotted against the corresponding buffer pH. Calibration points were fitted with a sigmoidal curve given in the text below.

Table 10 Calibration points obtained from transformed yeast strains of *Saccharomyces cerevisiae*. Calibration points were used for construction of calibration curves. Corrected values are presented.

plasmid	pHl-U	pHl-U	pHl-G	pHl-U
cytosolic pH	**Sc1 WT**	**Sc2 WT**	**Sc2 WT**	**Sc2 Nha1Δ**
5,5	0,41 ± 0,02	0,43 ± 0,01	0,46 ± 0,01	0,42 ± 0,01
6,0	0,52 ± 0,04	0,56 ± 0,01	0,57 ± 0,01	0,57 ± 0,01
6,5	0,80 ± 0,06	0,83 ± 0,01	0,81 ± 0,05	0,83 ± 0,01
7,0	1,14 ± 0,08	1,16 ± 0,02	1,14 ± 0,05	1,12 ± 0,02
7,5	1,45 ± 0,09	1,50 ± 0,03	1,34 ± 0,10	1,54 ± 0,03
8,0	1,71 ± 0,09	1,76 ± 0,05	1,52 ± 0,20	1,86 ± 0,08
replicates	14	12	8	12

Table 11 Calibration points obtained from transformed yeast strains of Zygos*accharomyces cerevisiae*. Calibration points were used for construction of calibration curves. Corrected values are presented.

plasmid	pHl-U	pHl-U	pHl-U	pHl-U
cytosolic pH	**Zr WT**	**Zr Nha1Δ**	**Zr Sod2-22 Δ**	**Zr Nha1Δ Sod2-22 Δ**
5,5	0,44 ± 0,01	0,44 ± 0,01	0,44 ± 0,01	0,43 ± 0,01
6,0	0,59 ± 0,01	0,57 ± 0,01	0,57 ± 0,01	0,56 ± 0,02
6,5	0,80 ± 0,01	0,79 ± 0,01	0,78 ± 0,01	0,78 ± 0,01
7,0	1,12 ± 0,02	1,13 ± 0,03	1,09 ± 0,03	1,12 ± 0,02
7,5	1,46 ± 0,02	1,46 ± 0,05	1,41 ± 0,07	1,46 ± 0,03
8,0	1,70 ± 0,03	1,72 ± 0,06	1,64 ± 0,10	1,70 ± 0,04
replicates	10	8	8	8

By comparison among different transformed strains we have come to the conclusion that calibration curves are almost identical (in the range of obtained experimental errors) for both yeast species (see tables 10 and 11). This means that cytosol in both species behaves in a very similar manner with respect to its impact on pHluorin. Beside this we have decided to use one single and unique calibration curve for every strain and for every mutation performed to suppress experimental errors.

Extrapolation of calibration was performed by fitting the calibration points with the following sigmoidal function:

$$R_{410/470} = \frac{I_{\max} \cdot pH^{nH}}{K_{0,5}^{nH} + pH^{nH}} + konst$$

Crucial for obtaining correct and reproducible calibration curves is to set the experimental parameters properly. We discuss this topic more closely in following sections.

3.1.4. Adjustment of incubation time

Properly adjusted time of incubation in calibration buffer should guarantee that cytosol and calibration buffer achieve a stable state, when cytosolic pH equals the extracellular pH. This cannot be proofed directly, thus fluorescence ratio $R_{410/470}$ has to be monitored during the incubation. After a given time at equilibrium state, fluorescence ratio $R_{410/470}$ remains essentially stable.

To identify proper incubation time, wild type strains *Sc2 WT* was resuspended in calibration buffers titrated to six different pH values. Fluorescence ratios were monitored during the whole incubation in calibration buffer (approximately *10* minutes for *Sc2 WT*). Results are presented in the figure *12*. The same procedure was repeated also for *Zr* WT, it was proofed that longer incubation time of *15* minutes for is necessary (results are not presented in graphical form).

To quantify the dependence of properly adjusted incubation time on calibration curve, experiments monitoring the fluorescence ratio $I_{410/470}$ directly after the resuspension of *Sc2 WT* in calibration buffer and after *10* minutes were performed. Corresponding calibration curves were then constructed (see figure 13). Significant differences are visible. Calibration curve obtained directly after resuspension lies over the curve obtained after *10* minutes of incubation.

Using small incubation times would therefore return systematic errors. According to figure 13, fluorescence ratio 1,0 returns cytosolic pH of approximately *6,6* by using small incubation time and approximately *6,8* by using longer incubation time. An error of approximately *0,2* units would be the result. This is comparable to the effect of correction.

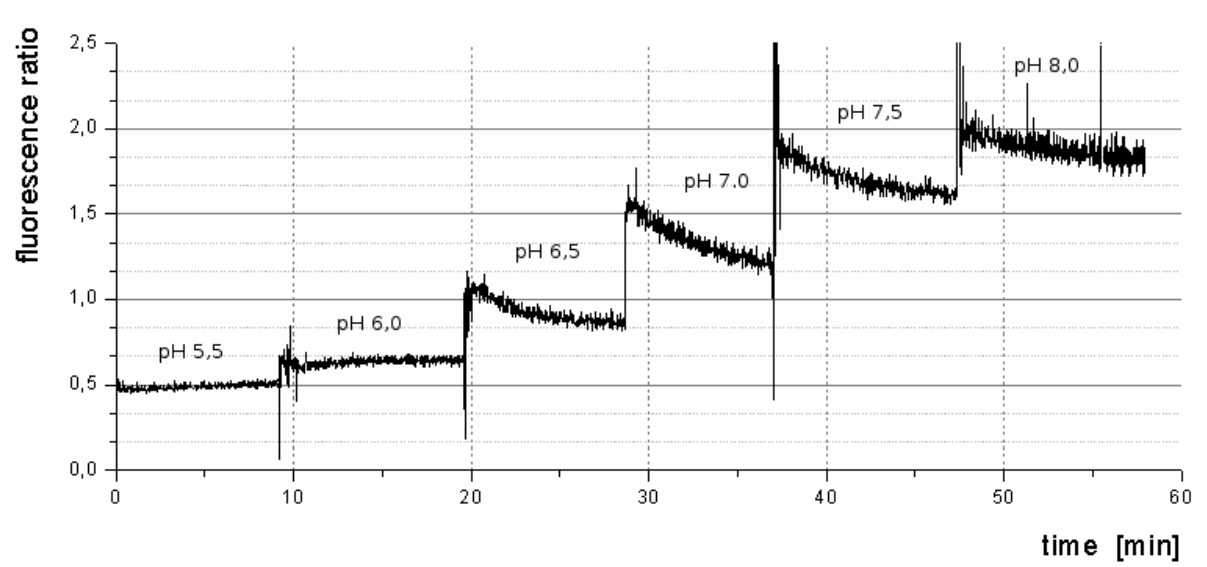

Figure 12 Time dependence of uncorrected fluorescence ratio $I_{410/470}$ in calibration buffer without ionophores. Two biological replicates of *Sc1* W*T* strain were averaged. Fluorescence ratio was measured directly after resuspension of yeast cells in calibration buffer. The x-axis shows the time progression of the measurement. Peaks are artefacts caused by changing the samples. The given pH values represent extracellular pH.

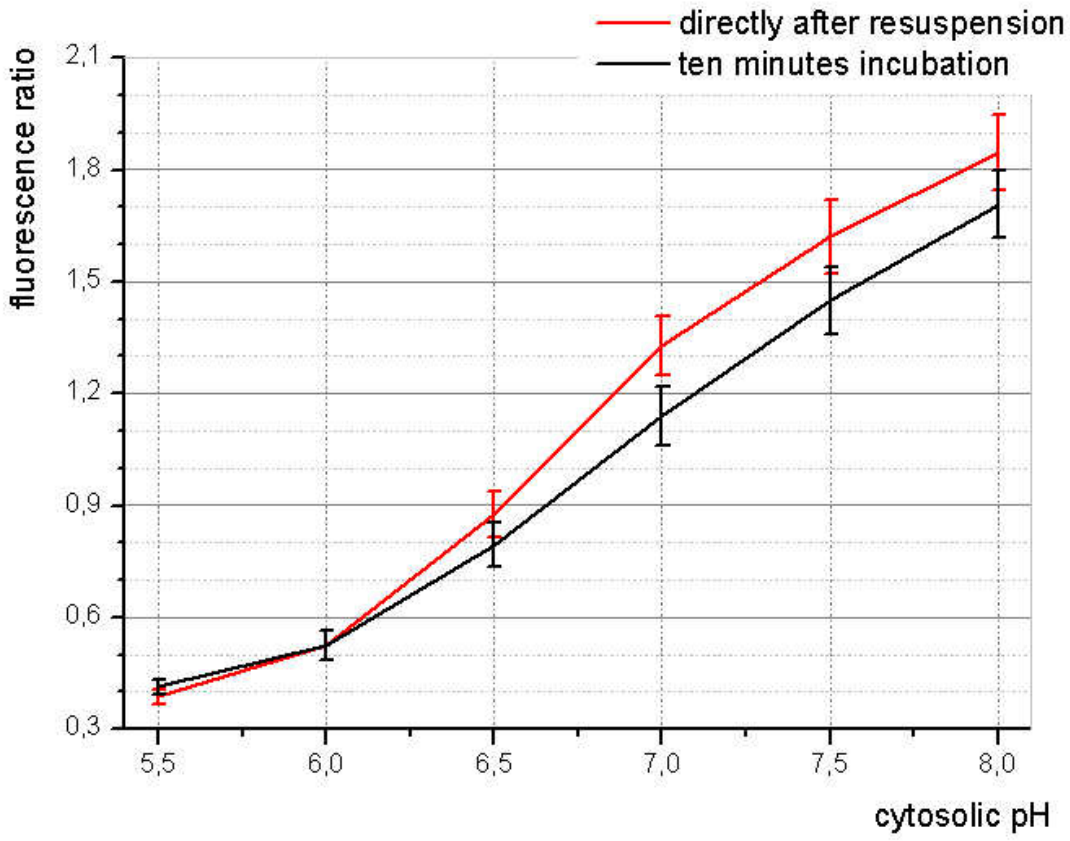

Figure 13 Calibration curves obtained directly after resuspension of *Sc2 WT* in calibration buffer (without ionophores) and after *10* minutes of incubation in calibration buffer (without ionophores).

3.1.5. The impact of ionophores on calibration

To date, several groups [9,12,39] performed calibrations in buffers containing compounds as described in table 7. Originally, the calibration method was developed by Brett et al [9]. Martínez-Muñoz & Kane used also the same approach [39]. Only Marešová et al, used an alternated variant of calibration buffer, where ionophores were omitted. They believed, ionophores did not exhibit any impact on calibration [12].

A different approach of pHluorin signal calibration was used by Orij et al [11]. Yeast cells were incubated in PBS containing digitonin at *100 μg/ml* concentration. After ten minutes of incubation yeast was resuspended in citric acid buffers of desired pH, where also the calibration itself was performed. Since the correct calibration of pHluorin signal is crucial for measuring correct cytosolic pH values, the importance of ionophores has to be investigated more closely. Thus, we have performed several experiments involving modification in composition of calibration buffers (without or with selected ionophores) at different incubation times.

Calibration buffers were prepared as described in table 7. The effect of four different ionophores on calibration curves was tested. Two different concentrations of the combination monensin and nigericin have been tested. In each case, two types of incubation times were tested (incubation time of *10* minutes and directly after the resuspension of yeast).

Table 12 Four types of ionophores were used, two of them were combined and used in two different combinations.

	Description of modification	**Ionophore concentration**
1	addition of nigericin and monensin	Nigericin: *5 μM* monensin: 38 *μM*
2	addition of nigericin and monensin	Nigericin: *10 μM* Monensin: *75 μM*
3	addition of digitonin	Digitonin: 1*00 μg/ml*
4	addition of ODDC	ODDC: *10 μM*

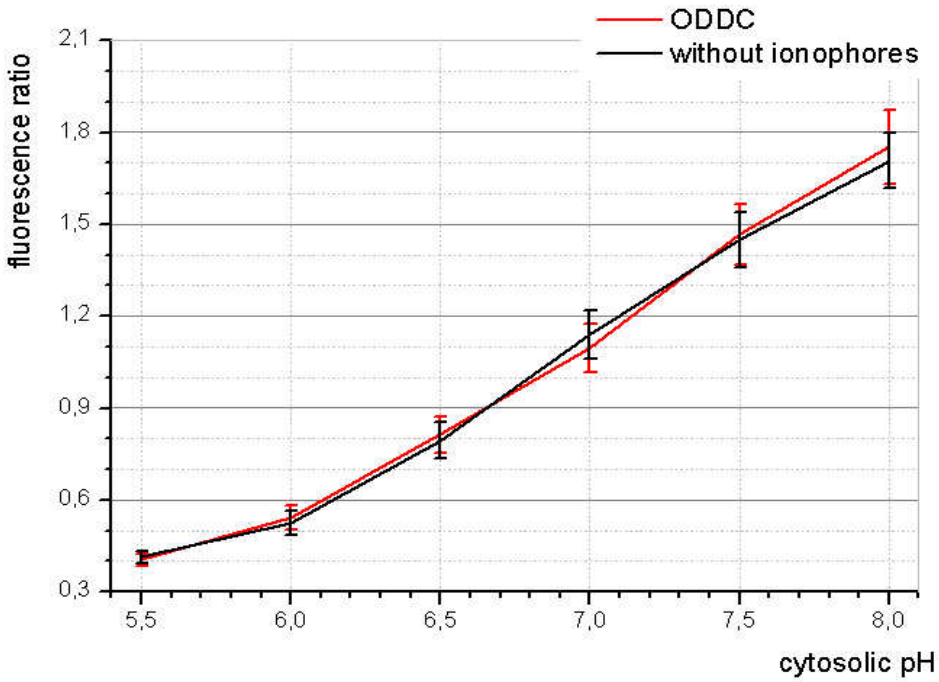

Figure 14 Comparison of calibration curves obtained with a ionophore ODDC and without ionophores. Both calibrations were acquired after 10 minutes of incubation. ODDC was added to the calibration buffer at *10 μM* concentration. Calibration curves were corrected.

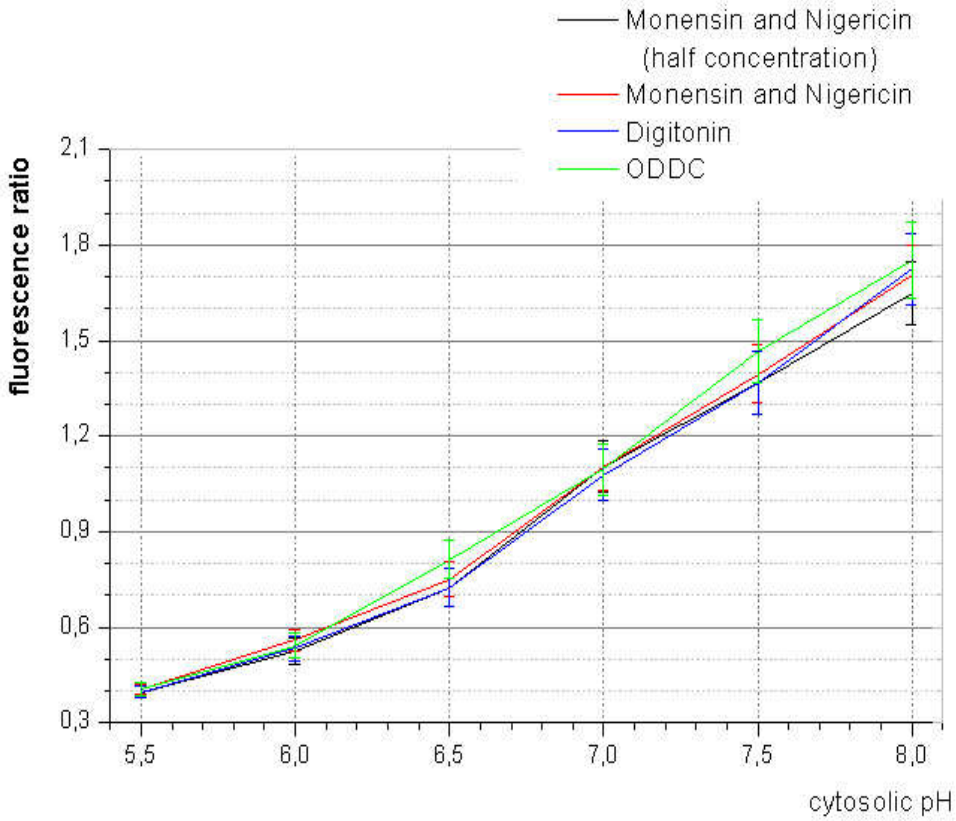

Figure 15 Calibration curves for different ionophores show only an insignificant spread of values compared to each other. Calibration curves were corrected

3.1.6. Calibration curves for yeast transformed by pHl-U and pHl-G

Insertion of plasmids encoding pHluorin and a selection marker induces new properties into selected yeast strain. Gene encoding pHluorin enables us to measure cytosolic pH via fluorescence and selection marker is required to select only transformed yeast. In this work selection marker *ura3* encoding proteins required for uracil synthesis was used. Yeast transformed by plasmid encoding *ura3* is capable to synthesize uracil and thus grow on media without uracil. On the other hand, uracil synthesis could have an impact either on cytosolic pH or pHluorin itself. Therefore, plasmid pHl-G was constructed, where *ura3* was replaced and a selection marker inducing geneticin resistance was added (see section 2.1.). Subsequently yeast of strain *Sc2 WT* was grown according to section 2.1.2.

Comparison between transformation with pHl-U and pHl-G revels (see figure 16) that both curves are almost identical within the range of experimental error, but calibration curve of yeast transformed by pHl-G shows significantly larger errors due to higher signal-to-noise ratio. We also conclude that both curves differ only because of small expression of pHluorin in yeast transformed by pHl-G.

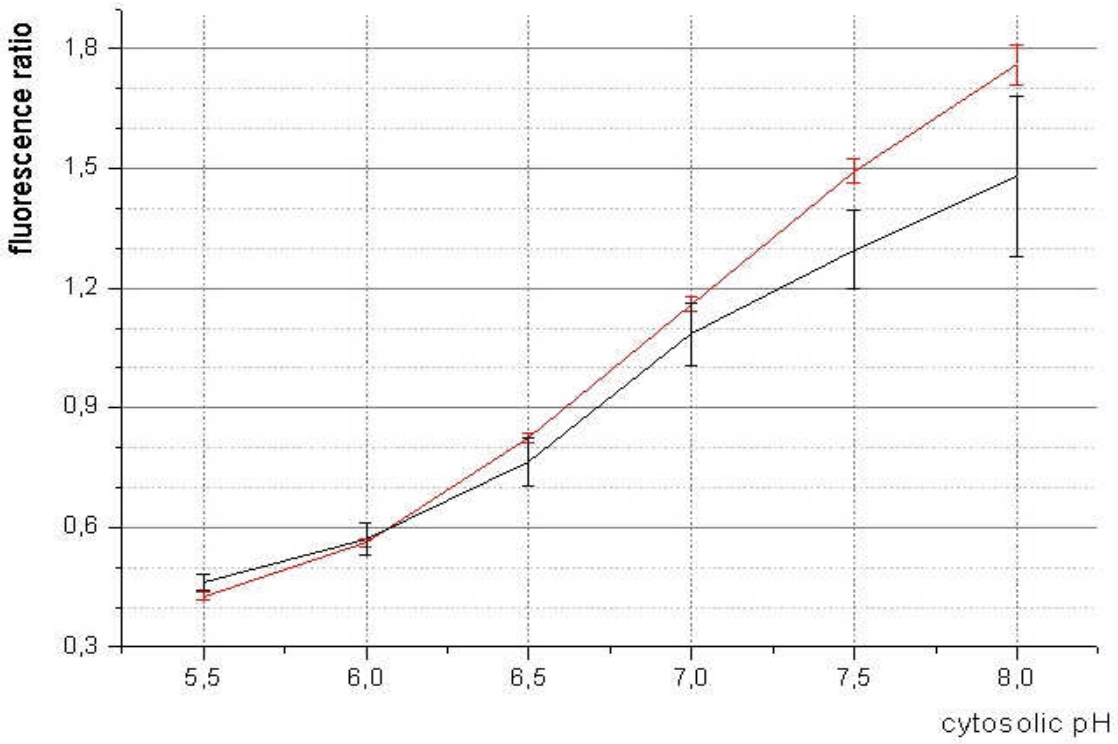

Figure 16 Corrected calibration curves obtained for *Sc1 WT* transformed by pHl-U (red) or pHl-G plasmid (black). Error bars obtained for pHl-G are larger because of lower fluorescence signal acquired. Both curves are not exactly identical, but this is partially caused by e large experimental error in the case of pHl-G.

3.2. Cytosolic pH in Saccharomyces cerevisiae

To explore the interdependence between cytosolic pH and sodium transport, wild type yeast (*Sc1 WT* and *Sc2 WT*) and *nha1* deletion mutants were prepared. To ensure that pHluorin expression was successful, excitation fluorescence spectra from *Sc*1 *WT* were acquired (see figure 17). To determine whether pHl-G plasmid is suitable for pH measurement, yeast was transformed by pHl-G and cytosolic measurements were performed (3.2.1.). Comparison to yeast transformed by pHl-U revealed that expression of pHluorin from pHl-G is lower. From this reason, a larger ratio of signal-to-noise was obtained. From this reason, pHl-U plasmid was employed for further measurements. The impact of Nha1p on cytosolic pH was studied under several environmental conditions such as different extracellular concentration of H^+, K^+ and Na^+ (see section 3.2.2.). Addition of glucose revealed further effects related to the interdependence between Nha1p and cytosolic pH (see section 3.2.3.). In accordance to Maresova et al (2010), we have determined the buffering capacity for *Sc2 WT* and *Sc2 Nha1Δ* (see section 3.2.4.), so the mechanisms contributing to regulation of cytosolic pH could be quantified.

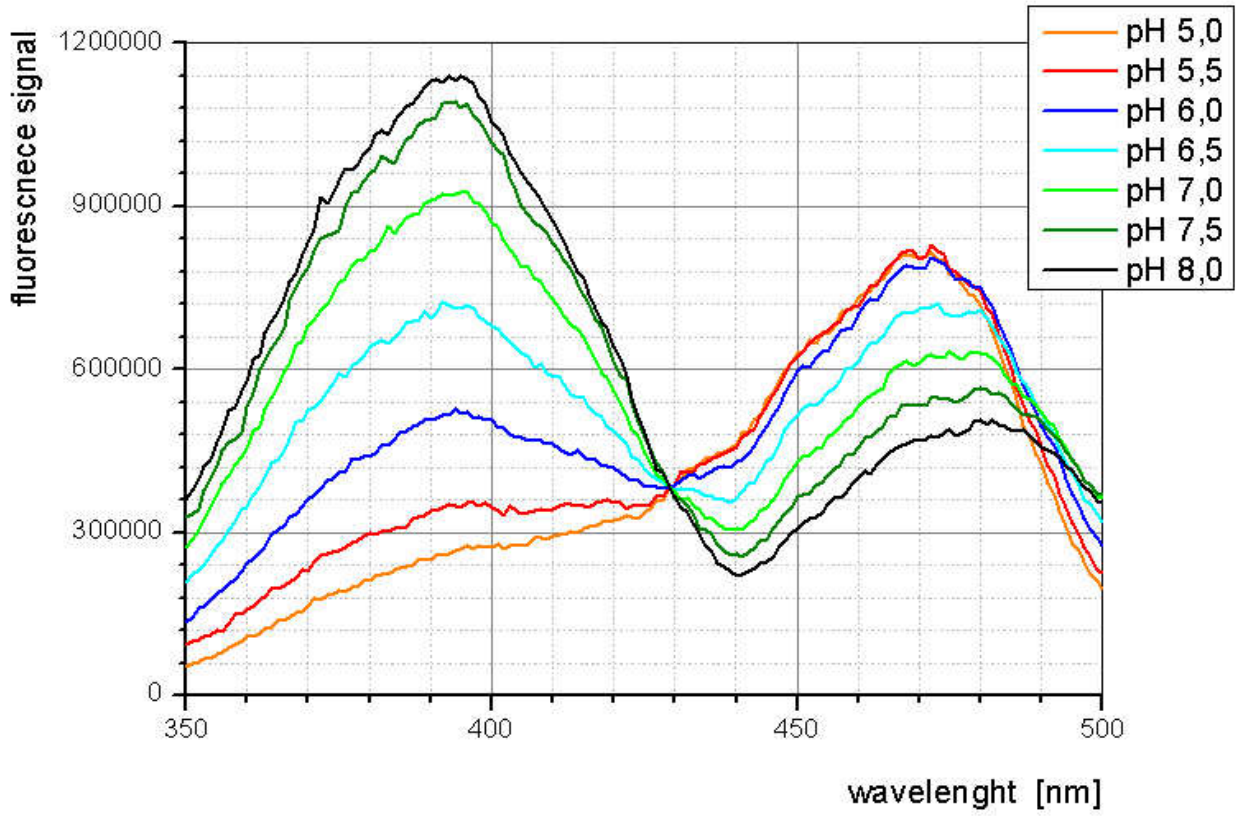

Figure 17 Emission spectra of pHluorin from Saccharomyces cerevisiae. Strain BY4741 carrying pHl-U plasmid was incubated in calibration buffer without ionophores. Background correction was performed. Spectra were renormalized at isobestic point (approximately *429 nm*). Three biological replicates have been measured and averaged.

3.2.1. Measurements of cytosolic pH by using pHl-G plasmid

Transformation with pHl-U requires yeast strain with specific auxotrophic mutations (deletion of *ura3*). But it can be problematic to compare yeast strains with two different auxotrophies to each other. Therefore, the *Sc1 WT* strain was transformed by pHl-G and pHl-U plasmid. A broad range of environmental conditions was employed figure 18).

Cytosolic pH obtained for yeast growing on YNB with uracil is larger than in yeast growing without uracil, but two problematic points emerge. First, large experimental errors were obtained for yeast transformed by pHl-G (yeast growing in YPD or in YNB with uracil). Second, errors calculated as standard deviations do not include experimental errors of calibration. But in section 3.1.6., we have shown that transformation with pHl-G leads to smaller signal-to-noise ratio. We have also performed T-tests (with pHl-U as reference), which demonstrated low significance (T-test for pHl-G in YPD returned 25%, for pHl-G in YNB with uracil 41%). Thus, we conclude that increased cytosolic pH in yeast transformed by pHl-G is only an artefact. Subsequently only transformation with pHl-U plasmid was used for further measurements.

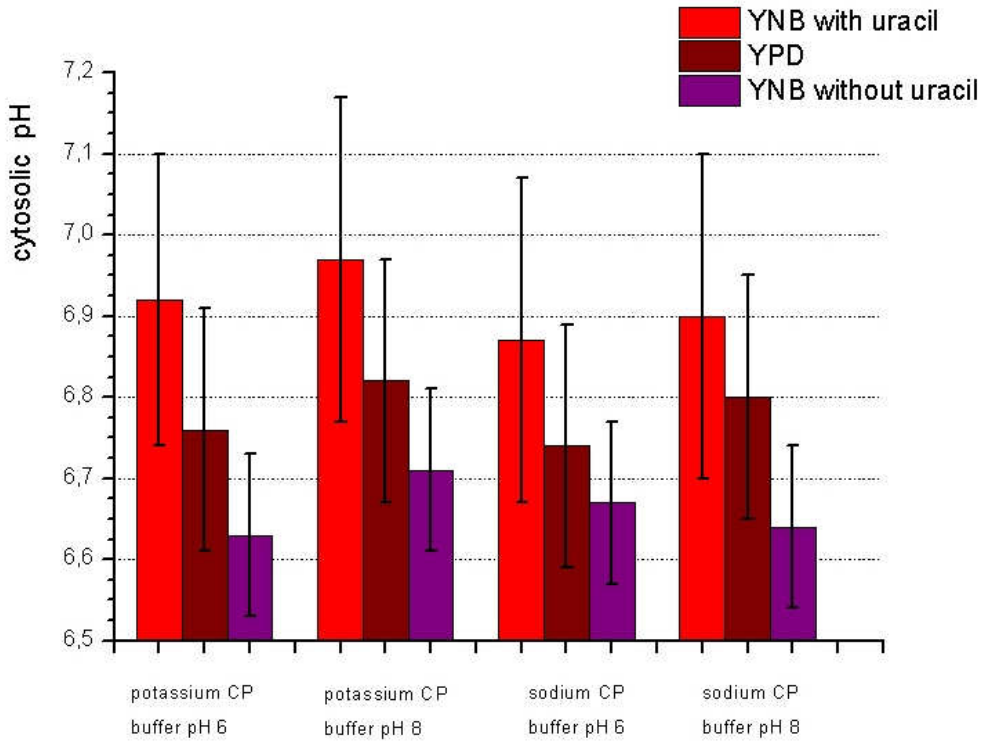

Figure 18 Cytosolic pH of yeast strain BY4741 transformed either with pHl-U or pHl-G. Yeast transformed by pHl-U was grown only in YNB, yeast transformed by pHl-G was grown in YPD (wine-coloured column) and YNB containing uracil (red-coloured column). Yeast was deprived of energy sources for about 30 minutes. At least six replicates for each measurement were used.

3.2.2. Cytosolic pH in the absence of energy sources

To determine the role of Nha1p in regulation of cytosolic pH, wild type strain *Sc2WT* and deletion mutant *Sc2 Nha1Δ* (transformed by pHl-U) were exposed to several environmental conditions. Yeast was harvested in mid-exponential phase and cut from energy supply due to several necessary procedures for about *45* minutes before the measurement.

Cytosolic pH of yeast (without supply of energy sources) was determined to be approximately *6,6* units. Wild type yeast and deletion mutant exhibit no significant differences except of sodium buffer at pH *6*, where a difference of approximately *0,15* units was observed. The difference lies within the range of experimental error (also T-test returned 9%). Thus, only restricted conclusions can be made. An increased cytosolic pH of approximately *0,1* units can be observed, when comparing potassium buffers at pH at *6* and *8*. But as before, the effect lies within the range of experimental error.

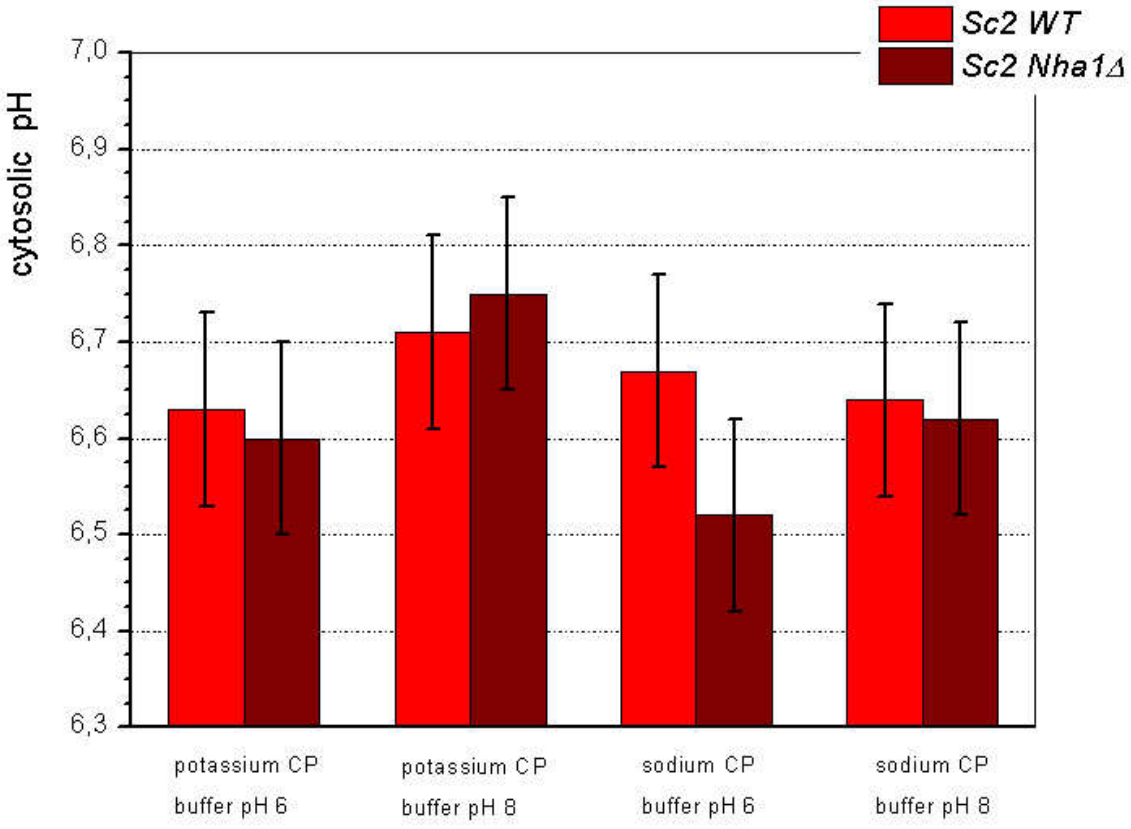

Figure 19 Cytosolic pH in *Sc2 WT* and *ScNha1Δ* under several environmental conditions No energy sources were available for about *45* minutes before the measurement. In the case of *Sc Nha1Δ* in sodium CP buffer at pH 6, a decreased cytosolic pH was be observed. At least *10* biological replicates were used.

3.2.3. Cytosolic pH after addition of glucose

A deprivation of energy sources for *45* minutes was proofed to result in decreased cytosolic pH. It is therefore expected that addition of glucose causes further effects, which may give insight into the interdependence between Nha1p and cytosolic pH. For this purpose, wild type strain *Sc2WT* and deletion mutant *Sc2 Nha1Δ* (transformed by pHl-U and harvested in mid-exponential phase) were used.

Both yeast strains show an increased cytosolic pH after addition of glucose (figure 20). This effect is known as glucose effect (Orij et al 2008). Mutants with deleted *Nha1* show a smaller decrease of approximately 0,3 units in potassium CP buffer and *0,5* units in sodium CP buffers. Wild type strain displayed also a significant dependence of cytosolic pH on extracellular pH, cytosolic pH in sodium CP buffer was increased by approximately *0,2* units compared to potassium CP buffer. Strains with deleted *Nha1* exhibit also a minor dependence of cytosolic pH on extracellular pH, but the effect is small (approximately *0,1* units) and lies within the range of experimental error.

In the case of *Sc2 WT*, also time-resolved measurements of glucose effect (figure 21) were performed. First, yeast was incubated for *10* minutes in CP buffer at pH 8,0. A stable cytosolic pH of approximately *6,7* units was observed, then glucose was added. After transient acidification at the beginning, rapid alkalinization followed and within only *5* minutes cytosolic pH increased to approximately *7,4* units.

Comparison with Orij et al [11] reveals the same qualitative results. On the other hand, slightly different quantitative parameters were observed. First of all, *45* minutes long starvation resulted in cytosolic pH of approximately *6,7* units, whereas two hours long starvation performed by Orij et al [11] resulted in pH of *6,0* units. Therefore, we conclude that after *45* minutes only a state of partial starvation was achieved. This hypothesis is supported also by time dependence of the observed glucose effect. We have observed that yeast gained a stable cytosolic pH of *7,4* after approximately *5* minutes, whereas Orij et al [11] observed a much longer time of approximately one hour.

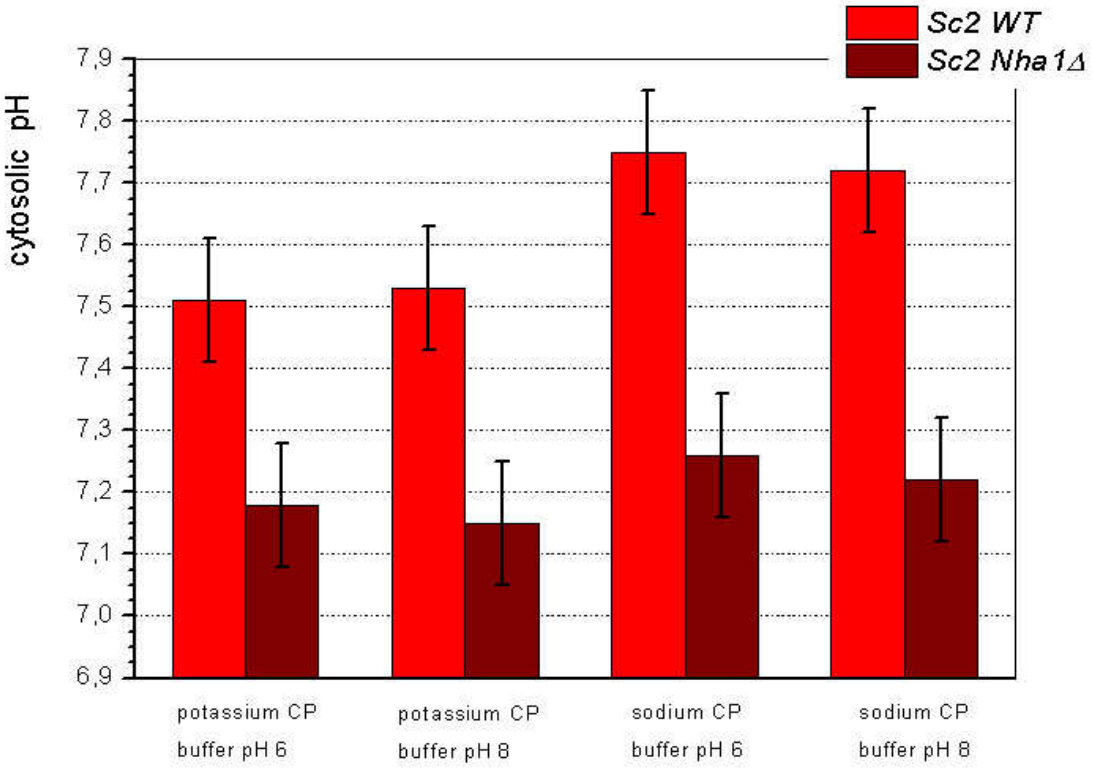

Figure 20 Cytosolic pH in *Sc2 WT* and *Sc Nha1Δ* after incubation with 0,2% glucose. The values were obtained in two different CP buffers at different values of external pH. The picture shows a significant decrease of cytosolic pH in yeast with deleted sodium transporter *Nha1*.

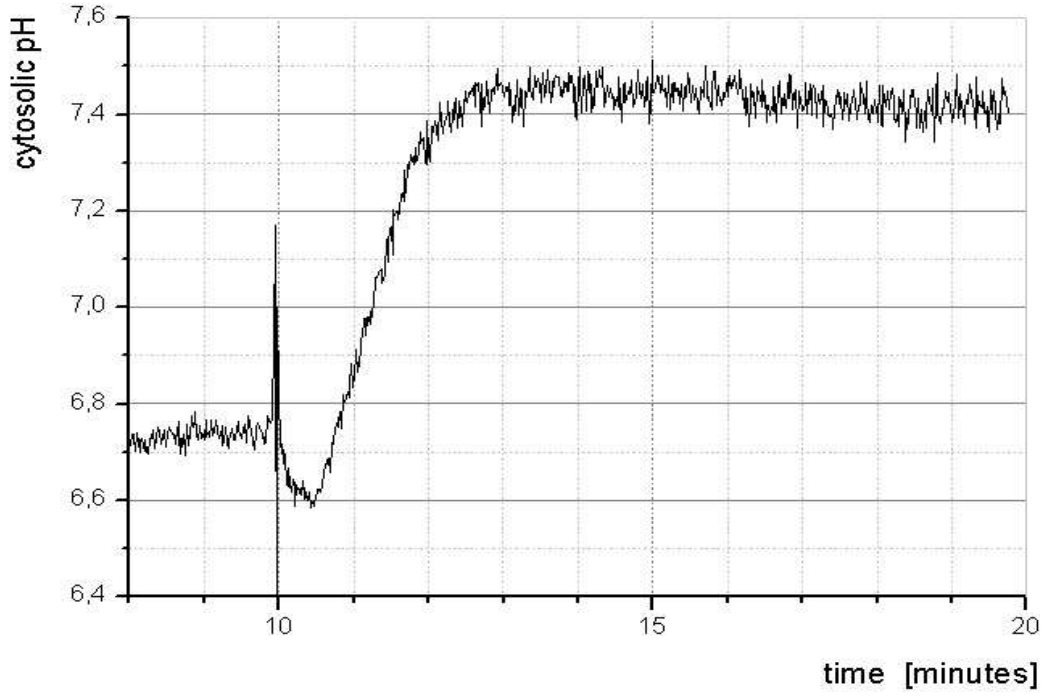

Figure 21 Time resolved glucose effect in CP buffer at pH *8,0*. Immediately after the addition of glucose a transient alkalinization of approximately *0,1* units was observed, then within approximately *5* minutes a stable plateau of approximately *7,4* units was maintained. Measurements from three biological replicates of *Sc2 WT* (transformed by pHl-U) were averaged. Error bars of approximately *±0,1* units were estimated as standard deviations and are not shown because of readability of the graph.

3.2.4. Buffering capacity

To explore the impact of Nha1p on buffering capacity, several environmental conditions were applied to both: wild type yeast and *Sc2 Nha1Δ*. The dependence on the presence of glucose was explored by determining buffering capacity after incubation with *0,2%* glucose.

Measurements without supply of glucose (see table 13) revealed that potassium and sodium concentrations did not influence the buffering capacity significantly. Only resuspension of *Sc2 Nha1Δ* in sodium CP buffer revealed an increase of buffering capacity. A much larger impact was caused by the presence of glucose (see table 14). In the absence of glucose buffering capacity of approximately *40 mM* was observed, whereas in the presence of glucose buffering capacity decreased to approximately *15 mM*.

Table 13 Buffering capacity of selected yeast strains after approximately one hour of energy source deficiency.

	Sc1 WT	**Sc2 WT**	**Sc2 Nha1Δ**
potassium buffer	39 ± 8 *mM*	44 ± 10 *mM*	41 ± 4 *mM*
sodium buffer	35 ± 10 *mM*	32 ± 6 *mM*	56 ± 4 *mM*
biological replicates	3	4	4

Table 14 Buffering capacity of selected yeast strains after 10 minutes long incubation in citrate-phosphate buffer containing 0,2% glucose.

	Sc1 WT	**Sc2 WT**	**Sc2 Nha1Δ**
potassium CP buffer with 0,2% glucose	13 ± 4	11 ± 3	17 ± 3
sodium CP buffer with 0,2% glucose	16 ± 6	18 ± 4	17± 4
biological replicates	3	4	4

3.3. Cytosolic pH in Zygosaccharomyces rouxii

To explore the interdependence between cytosolic pH and sodium transport, wild type yeast (*Zr WT*) and mutants with affected sodium transport were employed. To ensure that pHluorin expression was successful, excitation fluorescence spectra from *Zr WT* were acquired (figure 22).

The impact of Nha1p and Zr Sod2-22p on cytosolic pH was studied under several environmental conditions (such as different extracellular concentration of H^+, K^+ and Na^+), for details see section 3.3.1. Addition of glucose revealed also further effects (section 3.3.2.). In accordance to Maresova et al [12], we have estimated the buffering capacity for all employed yeast strains of *Zygosaccharomyces rouxii* (see section 3.3.3.), so the mechanism of cytosolic pH regulation could be quantified.

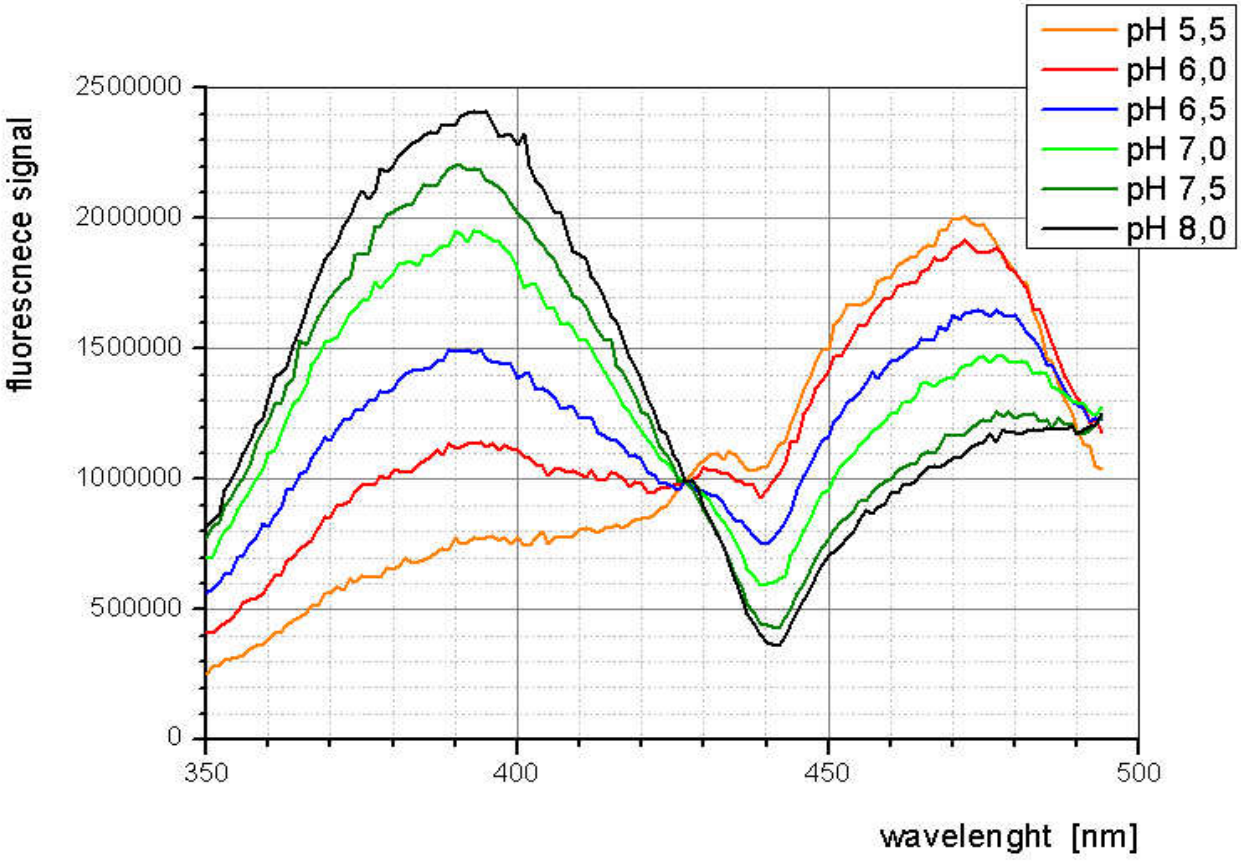

Figure 22 Emission spectra were obtained from living yeast of *Zygosaccharomyces rouxii*, the strain *Zr WT* was used. Three biological replicates have been measured. The obtained spectra have been averaged and renormalized to give the same fluorescence signal in the isobestic point (approximately 427 nm). The background fluorescence signal was subtracted.

3.3.1. Cytosolic pH in the absence of energy sources

To explore the interdependence of sodium transport and cytosolic pH, wild type strain *Zr WT* and mutants with affected sodium transport (all transformed by pHl-U) were exposed to several environmental conditions. Yeast was harvested in mid-exponential phase and cut from energy supply due to several necessary procedures for about *45* minutes before the measurement.

Wild type yeast and deletion mutants displayed no significant differences in cytosolic pH (see figure 23). The only exception were mutant strains *Zr Nha1Δ* and *Zr Nha1Δ Sod2-22Δ* in sodium buffer at pH *6*, where a difference of approximately *0,15* units was observed. For the mutant strain *Zr Nha1Δ* the difference lies within the range of experimental errors (also the T-test returned 10%), but in the case of *Zr Nha1Δ Sod2-22Δ* a significant difference was observed (T-test returned 1%), Interestingly there is almost no difference between *Zr Nha1Δ* and *Zr Nha1Δ Sod2-22Δ* in sodium buffer at pH *6*.

An increase of approximately *0,1* units of cytosolic pH was observed in potassium CP buffer. But as with the previous observation, the effect lies within the range of experimental error. The value of cytosolic pH in potassium CP buffer at *pH of 6,0* and in sodium CP buffer at *8,0* are approximately the same for both yeast strains. The value of approximately *6,6* units was determined.

By comparison of potassium buffer of pH *8,0* to the same type of buffer at pH *6*, an increase of approximately *0,1* units can be observed for all yeast strains. The effect lies partially within the range of experimental error. The values of cytosolic pH in potassium CP buffer at *8,0* and in sodium CP buffer at pH *6,0* eventually *8,0* are approximately the same for all yeast strains (without the previously described exception of *Zr Nha1Δ* and *Zr Nha1Δ Sod2-22Δ* in sodium buffer of *6,0*) . Cytosolic pH of yeast *Zygosaccharomyces rouxii* (without supply of energy sources) was thus determined to be approximately *6,8* units and a dependence on environmental conditions was observed.

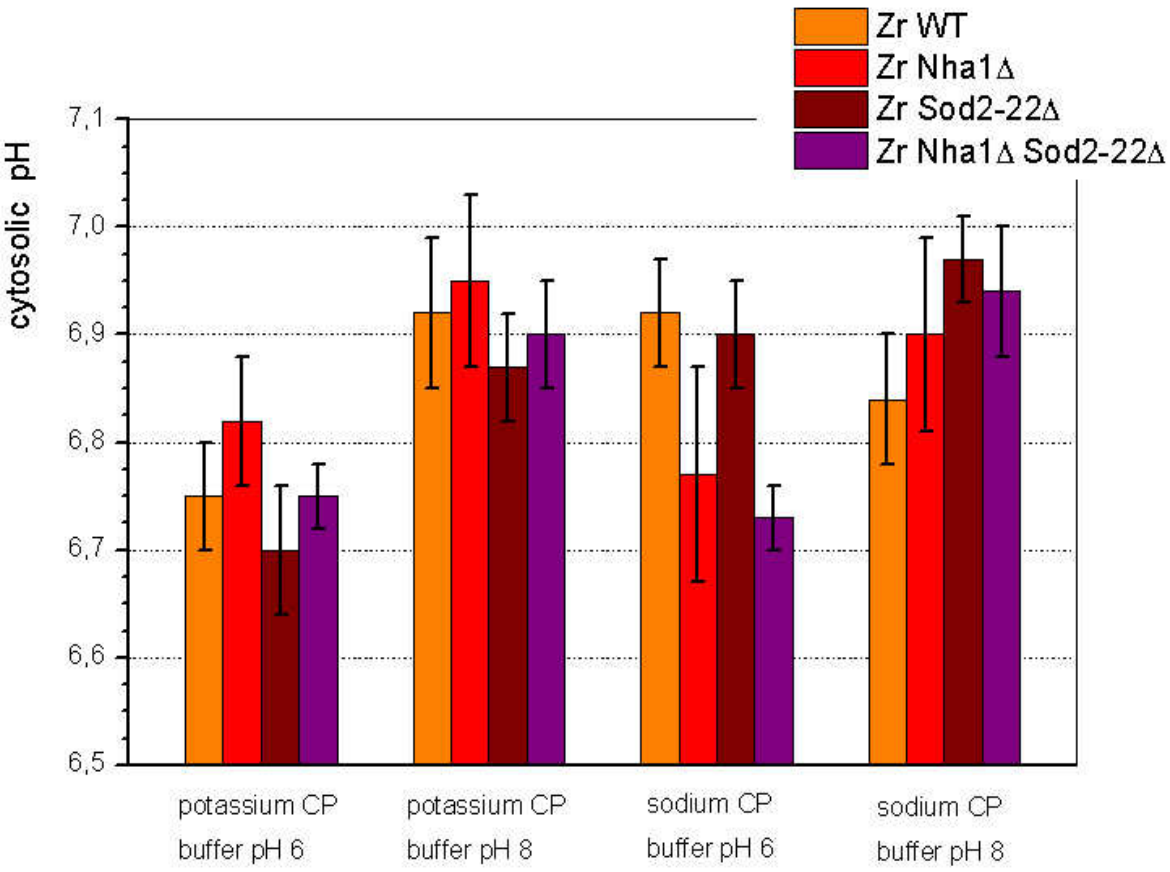

Figure 23 Cytosolic pH in wild type and three deletion mutants of *Zygosaccharomyces rouxii* (see the legend). Yeast strains were deprived of energy sources for about *45* minutes before the measurement No significant effects connected with different environmental conditions were observed. Only in the case of *Zr Nha1Δ* in sodium CP buffer at pH 6, a decreased cytosolic pH was observed. Error bars were obtained as standard deviations from at least six biological replicates.

3.3.2. Cytosolic pH in the presence of glucose

Deprivation of energy sources for *45* minutes was proofed to result in decreased cytosolic pH. It is therefore expected that addition of glucose causes further effects, which may give insight into the interdependence between sodium transporters and cytosolic pH. For this purpose, wild type strain *Zr2WT* and mutants with affected sodium transport (transformed by pHl-U and harvested in mid-exponential phase) were used. Yeast strains were incubated with glucose and time monitored measurements of cytosolic pH were performed. Measurements revealed essentially the same results as obtained for *Saccharomyces cerevisiae* in section 3.2.3.: after *15* minutes increased but stable cytosolic was achieved. From this reasons, incubation time of *15* minutes for all strains was employed.

According to figure 24, all yeast strain exhibit an increased cytosolic pH after the addition of glucose. This is known as glucose effect [11]. The increase of cytosolic pH is significantly larger in Zr *WT* than in deletion mutants. The difference is approximately *0,2* units in potassium CP buffer and *0,15* units in sodium CP buffers. No dependence of cytosolic pH on the type of CP buffer was observed. The only exception is the double mutant *Zr Nha1Δ Sod2*-22Δ, where a difference of approximately *0,1* units at extracellular pH of *6,0* is visible. The effect lies in the range of experimental error and has therefore a low significance. On the other hand, a significant increase of cytosolic pH with extracellular pH could be observed for the same yeast strain *Zr Nha1Δ Sod2*-22Δ. All other yeast strains show no evidence of such dependence.

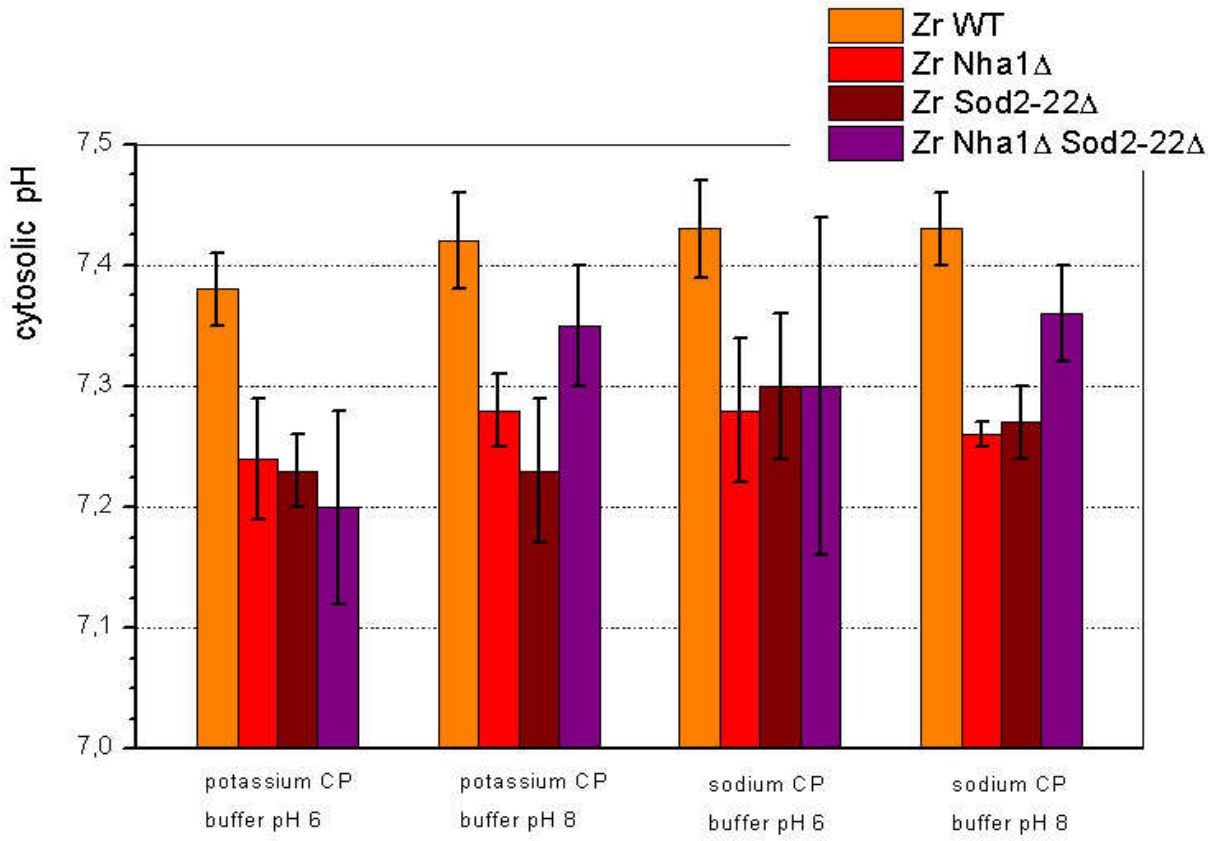

Figure 24 Cytosolic pH in wild type and three deletion mutants of *Zygosaccharomyces rouxii* (see the legend) after incubation in CP buffers with 0,2% glucose. Values were obtained in two different CP buffers at two different values of external pH. The picture shows a significant decrease of cytosolic pH in yeast with deleted sodium transporters *ZrNha1* or/and *ZrSod2-22*. Error bars were obtained as standard deviations.

3.3.3. Buffering capacity

To explore the impact of sodium transporters on buffering capacity, several environmental conditions were applied to the yeast strains. The dependence on the presence of glucose was explored by determining buffering capacity after incubation with *0,2%* glucose. Yeast was deprived of energy sources for about 45 minutes before the measurements.

In the absence of glucose no differences among the employed yeast strains were observed (table 15). Only in the case of *Zr Nha1Δ* a non-specific increase caused by experimental uncertainty (large experimental error) is visible. Because there was no comparable effect observed in *Zr Nha1Δ Sod2-22Δ*, we conclude it to be an artefact. Moreover, only four biological replicates were employed. From the same reasons, we conclude that the increase of buffering capacity in *Zr Nha1Δ* and *Zr Sod2-22Δ* supplied with glucose is rather a result of small statistical set, than a real effect of single gene deletion. Generally, buffering capacity was shown to decrease in the presence of glucose (tables 15 and 16).

Table 15 Buffering capacity of selected yeast strains after approximately one hour of energy source deficiency.

	Zr WT	**Zr Nha1Δ**	**Zr Sod2-22Δ**	**Zr Nha1Δ Sod2-22Δ**
potassium CP buffer	30 ± 7	60± 20	30 ± 10	32 ± 10
sodium CP buffer	29 ± 7	54 ± 17	34 ± 10	26 ± 5
biological replicates	6	4	4	6

Table 16 Buffering capacity of selected yeast strains after 15 minutes incubation in citrate-phosphate buffer containing 0,2% glucose.

	Zr WT	**Zr Nha1Δ**	**Zr Sod2-22Δ**	**Zr Nha1Δ Sod2-22Δ**
potassium CP buffer with 0,2% glucose	14 ± 10	38 ± 8	34 ± 10	13 ± 3
sodium CP buffer with 0,2% glucose	16 ± 10	34 ± 8	34 ± 10	20 ± 5
biological replicates	6	4	4	6

4. Discussion

4.1. Calibration

Experimental techniques used in this work are based on papers previously published by Brett et al [9], Martínez-Muñoz & Kane [39], and Marešová et al. [12]. All three groups have performed calibrations, which were based on the same calibration buffer. Marešová et al. omitted ionophores [12]. Remarkably, pHluorin expressed in different yeast strains gave rise to unique and different calibration curves for every yeast strain. Also values of cytosolic pH obtained by the three groups differ. Hence, we have systematically explored the role of ionophores for calibration.

Four different ionophores at usual concentrations were employed (section 3.1.5.), but no impact on calibration was observable. Thus, ionophores could not explain the differences. On the other hand, incubation time (section 3.1.4.) exhibited a significantly larger impact on calibration (approximately *0,2* units of cytosolic pH when recalculated). However, incubation time could not explain different calibration curves obtained after expression of pHluorin from different plasmids (pHl-U and pHl-G). Since low expression of pHluorin after transformation with pHl-G was the only one difference compared to transformation with pHl-U, possible background and parasitic fluorescence from calibration buffer were more closely investigated.

Excitation spectra of pure calibration buffer were compared to excitation spectra of pHluorin and a relative high noise-to-signal ratio was discovered (section 3.1.1.). Thus, correction to the background signal was necessary. After applying corrections to yeast transformed by pHl-G and pHl-U both curves have overlapped essentially. In the case of pHl-G, a correction of approximately *0,6* units of cytosolic pH was achieved. Correction of yeast transformed by pHl-U was shown to lie in the range of error caused by unsuitable incubation time, correction of approximately *0,2* units was achieved. Moreover, applying correction to all obtained calibration curves obtained within this work gave rise to similar calibration curves for both yeast species (*Saccharomyces cerevisiae* and *Zygosaccharomyces rouxii*). This is expected, when pHluorin does not interfere with the cell surrounding significantly.

The extent of correction was proofed to depend on the degree of pHluorin expression in yeast: the larger the expression of pHluorin the smaller was the correction. Different

expression of pHluorin may emerge due to several factors. In the case of pHluorin expressed from pHl-G, lower selection pressure enforced by geneticin can be significant. Thus, although both pHI-U and pHI-G contain the same promotor, lower selection pressure of geneticin causes that yeast requires less copies of pHI-G plasmids to be expressed and smaller expression of pHluorin is the result. Another reason may be physiological changes after deletion of selected gene. Thus, deletion mutants can express pHluorin differently compared to wild type yeast and different noise-to-signal ratio is the result. Therefore, by using uncorrected calibration curves, not only an error in absolute values of cytosolic pH is obtained, also systematic error will emerge, when one tries to compare yeast strains with different level of pHluorin expression.

To our knowledge, previously published results by Marešová et al. did not involve any corrections to background fluorescence [12], but systematic error seems to lie within the range of experimental error. This assumption is based on a good agreement of results obtained in this work with those published by Marešová et al. [12]. In the case of Brett et al, background subtraction to the scattering on yeast was performed [9]. Nevertheless, background subtraction with respect to signal of calibration medium was most probably not performed. This assumption is based on the use of normalization to the obtained calibration curves at pH *7*. This indicates that different calibration curves were obtained for each strain. Therefore, systematic errors arise by comparison among different yeast strains.

4.2. Cytosolic pH in wild type yeast strains

We have successfully determined cytosolic pH in wild type yeast of *Saccharomyces cerevisiae* and *Zygosaccharomyces rouxii*. For *Saccharomyces cerevisiae* deprived of energy sources for about *45* minutes a value of approximately *6,6* units was obtained. *Zygosaccharomyces rouxii* strain possessed a cytosolic pH of approximately *6,7* units under the same conditions. It seems that cytosolic pH is only slightly dependent of environmental pH in the range of pH 6 to pH 8. Also presence of sodium and potassium revealed only small differences.

For *Zygosaccharomyces rouxii*, no data were ever published to our knowledge, so no comparisons can be performed. In the case of *Saccharomyces cerevisiae*, several data were published. Values obtained from wild type strains of *Saccharomyces cerevisiae* are in a good

agreement with results published by Marešová et al. [12], Brett et al [9] and Martínez-Muñoz & Kane [39]. Remarkably, Orij et al have obtained cytosolic pH of approximately *6,0* units after 2 hours long starvation [11]. Consequently by comparing the results, we conclude that yeast is in a state of partial starvation after deprivation of energy sources for about *45* minutes.

This conclusion is also supported by time resolved measurements of glucose effect performed in wild type strain of *Saccharomyces cerevisiae* (figure 21). Obtained results were in good qualitative agreement to results published by Orij et al [11]: Shortly after addition of glucose, a transient alkalinization of cytosol followed by a rapid increase of pH was observed, but different quantitative parameters were determined. Orij et al observed an increase of cytosolic pH lasting for about *30* minutes before the stable value of approximately *7,4* units was achieved [11]. In our case, only approximately *5* minutes were necessary. Taken together for both yeast species, we have determined a value of approximately *7,6* units for *Saccharomyces cerevisiae* and *7,4* units for *Zygosaccharomyces rouxii*. Results obtained for *Saccharomyces cerevisiae* are in a good agreement with previously published results. The processes observed within the glucose effect are related to glycolysis and to function of two ATPases. The transient decrease of cytosolic pH at the beginning is explainable by processes involved in glycolysis. Then within seconds, Pma1p and V-ATPases are believed to be activated [11] and cytosolic pH increases therefore, until an equilibrium state of approximately *7,4* units is reached (see figure 21).

Measurements of cytosolic pH revealed also several differences between *Saccharomyces cerevisiae* and *Zygosaccharomyces rouxii*. First of all, measurements with glucose added to wild type strain of *Saccharomyces cerevisiae* have shown that cytosolic pH depends on extracellular concentration of potassium eventually sodium. But no similar effect could be observed in *Zygosaccharomyces rouxii*. Differences can be explained by higher salt-tolerance of *Zygosaccharomyces rouxii*.

Buffering capacity of cytosol was determined in both yeast species. In the absence of glucose, buffering capacity within the range of *30* to *40 mM per one unit* of pH was observed. In the presence of glucose the buffering capacity decreased to approximately *15 mM per one unit* in both yeast species. No significant dependence on the presence of either sodium or potassium cations in extracellular space could be proofed due to relative large errors. The decrease of buffering capacity is an artefact connected with the use of logarithmic

scale for H^+ concentration. Consequently, changing pH by one unit in the absence of glucose results in the change of free concentration of H^+ by approximately *220 nM* (from pH *6,6* to pH *7,6*). In the presence of glucose, free H^+ concentration changes by approximately 3*6 nM* (from pH *7,4* to pH *8,4*). Subsequently, recalculating the buffering capacity as the amount of strong base (acid) in *mM* required to change the concentration of free H^+ by *1 nM* gives following values: In the absence of glucose, approximately *0,15 mM* of strong base are required to raise the free H^+ concentration by *1 nM*. In the presence of glucose, approximately *0,4 mM* are necessary to increase the free H^+ concentration by *1 nM*.

Although still in the range of experimental errors, we have determined smaller values of buffering capacity (in *mM per one unit of* pH) than Marešová et al. [12]. This is not an effect of calibration correction since both the initial value and final value (after addition of strong base) of cytosolic pH during the measurements were corrected by almost the same value. More likely, this is caused only by experimental uncertainties.

4.3. Cytosolic pH in mutants with affected sodium transport

Mutant strains with affected sodium transport revealed insights into physiological interdependence between cytosolic pH and alkali-metal transport mediated by transporters homologous to Nha1. Remarkably, both yeast species exhibited a very similar behaviour. Deletion mutants deprived of glucose for about *45* minutes possessed a similar cytosolic pH in all types of CP buffers, when compared to wild type strains. Only the sodium CP buffer at pH 6 caused a decreased cytosolic pH in mutants lacking *Nha1p*. Since *Zygosaccharomyces rouxii* posses two different transport system for sodium, both the single deletion mutant of *nha1* gene and the double mutant with deleted *nha1* and *sod2-22* genes can be compared to each other. Remarkably, both deletion mutants exhibit almost the same decreased cytosolic pH, which can not be observed in the single deletion mutant of s*od2-22* gene. Thus, Nha1p seems to have a larger impact on cytosolic pH than Sod2-22p. On the molecular level, Nha1p is believed to be involved in activation of Pma1 ATPases. Thus, when *nha1* is not present, Pma1p is less active and a smaller proton efflux from cytosol takes place. Such an effect was not observed in potassium CP buffer at pH 6 due to the presence of a huge variety of potassium transporters, which positively activate Pma1p. At extracellular pH 8, the effect can not be observed due to proton gradient oriented inwardly into the cytosol.

After the addition of glucose to strains with affected sodium transport, even a more significant decrease of cytosolic pH could be estimated for both yeast species. All mutant strains possessed pH in the range of approximately *7,2* to *7,3* units, whereas wild type yeast possessed cytosolic pH of approximately *7,4* units for *Zygosaccharomyces rouxii* and *7,5* eventually *7,7* units for *Saccharomyces cerevisiae*. Similar measurements were performed by Brett et al (2005), but instead of increased cytosolic pH wild type yeast possessed a decreased cytosolic pH when compared with deletion mutants. However, these experiments (with glucose in APG) were performed in acidic environment at pH 2,7 and a large proton gradient oriented inwardly into cytosol was the result. Under such conditions, Pma1p ATPase can not effectively pump protons out of cytosol. Glucose is enters the cytosol of yeast by symport with Na^+. In wild type yeast, Nha1 transporters export Na^+ by antiport with H^+ and cytosolic pH decreases. In contrast, mutant strains lacking Nha1p cannot import H^+ and alkaline values of cytosolic pH are the result. In our case, environmental pH of 6 eventually 8 units was employed for measurements and thus, Pma1p ATPases cannot be omitted. Since Pma1p is positively activated by Nha1p, which is not expressed in mutant strains, proton efflux is less effective and acidification of cytosol is the result. Effect is observable in all types of CP buffers independently on the actual activity of Nha1p, because wild type yeast expresses it constitutively.

Since *Zygosaccharomyces rouxii* possess two transport systems for sodium, additional effects due to the action of *Sod2-22p* can be expected. But only in the case, when glucose was added to CP buffer at pH 8, a different behaviour of *Zygosaccharomyces rouxii* was observed. The double mutant *Zr Nha1Δ Sod2-22Δ* showed an increased cytosolic pH in comparison to single mutant strains. On the other hand, when compared to wild type strain, cytosolic pH was still decreased. Because at the molecular level, only little is known about *Sod2-22*, we restrict ourselves to assumption, that glucose and alkaline values of cytosolic pH may be involved in activation of *Sod2-22*.

In both yeast strains, the buffering capacity of mutant strains did not show any significant differences. Only in the case of *Zygosaccharomyces rouxii* mutants *Zr Nha1Δ* and *Zr Sod2-22Δ* supplied with *0,2%* glucose, increased buffering capacity was observed. However, this observation is inconsistent with the buffering capacity of double mutant strain *Zr Nha1Δ Sod2-22Δ*. This could mean that the actual experimental error was underestimated or systematic errors occurred. Therefore, a bigger statistical set of data should be acquired.

5. Conclusion

Measurements of cytosolic pH have been successfully performed using pH sensitive fluorescent protein pHluorin. It was shown that ionophores are redundant in calibration buffers and can be therefore omitted. Calibration buffers were proofed to give a significant background signal. Moreover, differences in pHluorin expression in different yeast strains lead to different ratios of background to pHluorin signal. Therefore, correction was necessary to clear the calibration from artificial impacts. Moreover, correction resulted in correct calibration curves (differences of *0,2 to 0,6* units) similar for yeast belonging to various yeast strains and yeast species. Corrected calibration curves did not depend on the expression level of pHluorin.

For the first time, cytosolic pH and buffering capacity of *Zygosaccharomyces rouxii* were determined. For the purpose of comparison, the same quantities were determined also for *Saccharomyces cerevisiae*. Studies were performed with wild type and mutants with affected sodium transport. Cytosolic pH of approximately *6,7* units was determined for *Zygosaccharomyces rouxii* in the absence of glucose. In the presence of glucose, an increased cytosolic pH of approximately *7,4* units was observed. Similar results were obtained also for *Saccharomyces cerevisiae*. It has been demonstrated that the buffering capacity of cytosol decreases in the presence of glucose in all yeast strains and yeast species studied. Moreover, the role of *Nha1* in pH homeostasis was shown to be almost identical for both yeast species. Generally, the Nha1p deletion resulted in acidification of cytosol, because Nha1p contributes to the activation of Pma1p (proton extrusion ATPase). The impact of *Zr Sod2-22* on pH homeostasis in *Zygosaccharomyces rouxii* was proofed to be less significant.

6. Bibliography

1. Goffeau, A.; Barrell, B. G.; Bussey, H.; Davis, R. W.; Dujon, B.; Feldmann, H.; Galibert, F.; Hoheisel, J. D.; Jacq, C.; Johnston, M.; Louis, E. J.; Mewes, H. W.; Murakami, Y.; Philippsen, P.; Tettelin, H.; Oliver, S. G. Life with 6000 genes. *Science* **1996,** *274* (5287), 546, 563-546, 567.

2. Sychrova, H. Yeast as a model organism to study transport and homeostasis of alkali metal cations. *Physiol Res.* **2004,** *53 Suppl 1*, S91-S98.

3. Sychrova, H. Yeast as a model organism to study transport and homeostasis of alkali metal cations. *Physiol. Res.* **2004,** *53* (Suppl 1), S91-S98.

4. Botstein, D.; Fink, G. R. Yeast: an experimental organism for modern biology. *Science* **1988,** *240* (4858), 1439-1443.

5. Barnett, J. A.; Payne, R. W.; Yarrow, D. Yeasts: Characteristics and identification. Cambridge University Press: 1983; pp 781-807.

6. de, M. J.; Straub, M.; Potier, S.; Tekaia, F.; Dujon, B.; Wincker, P.; Artiguenave, F.; Souciet, J. Genomic exploration of the hemiascomycetous yeasts: 8. Zygosaccharomyces rouxii. *FEBS Lett.* **2000,** *487* (1), 52-55.

7. Pribylova, L.; Papouskova, K.; Sychrova, H. The salt tolerant yeast Zygosaccharomyces rouxii possesses two plasma-membrane Na+/H+-antiporters (ZrNha1p and ZrSod2-22p) playing different roles in cation homeostasis and cell physiology. *Fungal. Genet Biol* **2008,** *45* (10), 1439-1447.

8. Arino, J.; Ramos, J.; Sychrova, H. Alkali metal cation transport and homeostasis in yeasts. *Microbiol Mol Biol Rev* **2010,** *74* (1), 95-120.

9. Brett, C. L.; Tukaye, D. N.; Mukherjee, S.; Rao, R. The Yeast Endosomal Na+(K+)/H+ Exchanger Nhx1 Regulates Cellular pH to Control Vesicle Trafficking. *Mol. Biol. Cell* **2005,** *16* (3), 1396-1405.

10. Martinez-Munoz, G. A.; Kane, P. Vacuolar and plasma membrane proton pumps collaborate to achieve cytosolic pH homeostasis in yeast. *J Biol Chem* **2008,** *283* (29), 20309-20319.

11. Orij, R.; Postmus, J.; Ter, B. A.; Brul, S.; Smits, G. J. In vivo measurement of cytosolic and mitochondrial pH using a pH-sensitive GFP derivative in Saccharomyces cerevisiae reveals a relation between intracellular pH and growth. *Microbiology* **2009,** *155* (Pt 1), 268-278.

12. Maresova, L.; Hoskova, B.; Urbankova, E.; Chaloupka, R.; Sychrova, H. New applications of pHluorin-measuring intracellular pH of prototrophic yeasts and determining changes in the buffering capacity of strains with affected potassium homeostasis. *Yeast* **2010,** *27* (6), 317-325.

13. Kinclova, O.; Potier, S.; Sychrova, H. The Zygosaccharomyces rouxii strain CBS732 contains only one copy of the HOG1 and the SOD2 genes. *J Biotechnol* **2001,** *88* (2), 151-158.

14. Kinclova, O.; Potier, S.; Sychrova, H. Difference in substrate specificity divides the yeast alkali-metal-cation/H(+) antiporters into two subfamilies. *Microbiology* **2002,** *148* (Pt 4), 1225-1232.

15. Goffeau, A.; Slayman, C. W. The proton-translocating ATPase of the fungal plasma membrane. *Biochim Biophys Acta* **1981,** *639* (3-4), 197-223.

16. Wohlrab, H.; Flowers, N. pH gradient-dependent phosphate transport catalyzed by the purified mitochondrial phosphate transport protein. *J Biol Chem* **1982,** *257* (1), 28-31.

17. Mellman, I. The importance of being acid: the role of acidification in intracellular membrane traffic. *J Exp Biol* **1992,** *172*, 39-45.

18. Alberty, R. A. Effects of pH in rapid-equilibrium enzyme kinetics. *J Phys Chem B* **2007,** *111* (50), 14064-14068.

19. Veine, D. M.; Arscott, L. D.; Williams, C. H., Jr. Redox potentials for yeast, Escherichia coli and human glutathione reductase relative to the NAD+/NADH redox couple: enzyme forms active in catalysis. *Biochemistry* **1998,** *37* (44), 15575-15582.

20. Whitten, S. T.; Wooll, J. O.; Razeghifard, R.; Garcia-Moreno, E. B.; Hilser, V. J. The origin of pH-dependent changes in m-values for the denaturant-induced unfolding of proteins. *J Mol Biol* **2001,** *309* (5), 1165-1175.

21. Dechant, R.; Binda, M.; Lee, S. S.; Pelet, S.; Winderickx, J.; Peter, M. Cytosolic pH is a second messenger for glucose and regulates the PKA pathway through V-ATPase. *EMBO J.* **2010,** *29* (15), 2515-2526.

22. Llopis, J.; McCaffery, J. M.; Miyawaki, A.; Farquhar, M. G.; Tsien, R. Y. Measurement of cytosolic, mitochondrial, and Golgi pH in single living cells with green fluorescent proteins. *Proc Natl. Acad. Sci U. S. A* **1998,** *95* (12), 6803-6808.

23. Kane, P. M. The where, when, and how of organelle acidification by the yeast vacuolar H+-ATPase. *Microbiol Mol Biol Rev* **2006,** *70* (1), 177-191.

24. Preston, R. A.; Murphy, R. F.; Jones, E. W. Assay of Vacuolar pH in Yeast and Identification of Acidification-Defective Mutants. *Proc. Natl. Acad. Sci. U. S. A* **1989,** *86* (18), 7027-7031.

25. Dubyak, G. R. Ion homeostasis, channels, and transporters: an update on cellular mechanisms. *Adv. Physiol. Educ.* **2004,** *28* (1-4), 143-154.

26. Nishimura, K.; Igarashi, K.; Kakinuma, Y. Proton gradient-driven nickel uptake by vacuolar membrane vesicles of Saccharomyces cerevisiae. *J Bacteriol* **1998,** *180* (7), 1962-1964.

27. Ohsumi, Y.; Anraku, Y. Active transport of basic amino acids driven by a proton motive force in vacuolar membrane vesicles of Saccharomyces cerevisiae. *J Biol Chem* **1981,** *256* (5), 2079-2082.

28. Paroutis, P.; Touret, N.; Grinstein, S. The pH of the secretory pathway: measurement, determinants, and regulation. *Physiology (Bethesda.)* **2004,** *19*, 207-215.

29. van Roermund, C. W.; de, J. M.; IJlst, L.; van, M. J.; Dansen, T. B.; Wanders, R. J.; Waterham, H. R. The peroxisomal lumen in Saccharomyces cerevisiae is alkaline. *J Cell Sci* **2004,** *117* (Pt 18), 4231-4237.

30. Seksek, O.; Bolard, J. Nuclear pH gradient in mammalian cells revealed by laser microspectrofluorimetry. *J Cell Sci* **1996,** *109 (Pt 1)*, 257-262.

31. Masuda, A.; Oyamada, M.; Nagaoka, T.; Tateishi, N.; Takamatsu, T. Regulation of cytosol-nucleus pH gradients by K+/H+ exchange mechanism in the nuclear envelope of neonatal rat astrocytes. *Brain Res* **1998,** *807* (1-2), 70-77.

32. Bracey, T. S.; Williams, A. C.; Paraskeva, C. Inhibition of radiation-induced G2 delay potentiates cell death by apoptosis and/or the induction of giant cells in colorectal tumor cells with disrupted p53 function. *Clin Cancer Res* **1997,** *3* (8), 1371-1381.

33. Dechant, R.; Binda, M.; Lee, S. S.; Pelet, S.; Winderickx, J.; Peter, M. Cytosolic pH is a second messenger for glucose and regulates the PKA pathway through V-ATPase. *EMBO J.* **2010,** *29* (15), 2515-2526.

34. Portillo, F.; Eraso, P.; Serrano, R. Analysis of the regulatory domain of yeast plasma membrane H+-ATPase by directed mutagenesis and intragenic suppression. *FEBS Lett.* **1991,** *287* (1-2), 71-74.

35. Ambesi, A.; Miranda, M.; Petrov, V. V.; Slayman, C. W. Biogenesis and function of the yeast plasma-membrane H(+)-ATPase. *J Exp Biol* **2000,** *203* (Pt 1), 155-160.

36. Alberts, B.; Johnson, A.; Lewis, J.; Raff, M.; Roberts, K.; Walter, P. *Molecular Biology of the Cell 4th ed.;* 4 ed.; Garland Science: New York and London, 2002.

37. Boyer, P. D. The ATP synthase--a splendid molecular machine. *Annu. Rev. Biochem.* **1997,** *66*, 717-749.

38. Forgac, M. Structure and function of vacuolar class of ATP-driven proton pumps. *Physiol Rev* **1989,** *69* (3), 765-796.

39. Martinez-Munoz, G. A.; Kane, P. Vacuolar and Plasma Membrane Proton Pumps Collaborate to Achieve Cytosolic pH Homeostasis in Yeast. *J. Biol. Chem.* **2008,** *283* (29), 20309-20319.

40. Portillo, F. Regulation of plasma membrane H(+)-ATPase in fungi and plants. *Biochim Biophys Acta* **2000,** *1469* (1), 31-42.

41. Nakamoto, R. K.; Rao, R.; Slayman, C. W. Transmembrane segments of the P-type cation-transporting ATPases. A comparative study. *Ann. N. Y. Acad. Sci* **1989,** *574*, 165-179.

42. Serrano, R. Structure and function of proton translocating ATPase in plasma membranes of plants and fungi. *Biochim Biophys Acta* **1988,** *947* (1), 1-28.

43. Serrano, R. In vivo glucose activation of the yeast plasma membrane ATPase. *FEBS Lett.* **1983,** *156* (1), 11-14.

44. Eraso, P.; Gancedo, C. Activation of yeast plasma membrane ATPase by acid pH during growth. *FEBS Lett.* **1987,** *224* (1), 187-192.

45. Seto-Young, D.; Perlin, D. S. Effect of membrane voltage on the plasma membrane H(+)-ATPase of Saccharomyces cerevisiae. *J Biol Chem* **1991,** *266* (3), 1383-1389.

46. Seto-Young, D.; Perlin, D. S. Effect of membrane voltage on the plasma membrane H(+)-ATPase of Saccharomyces cerevisiae. *J. Biol. Chem.* **1991,** *266* (3), 1383-1389.

47. Perlin, D. S.; Brown, C. L.; Haber, J. E. Membrane potential defect in hygromycin B-resistant pma1 mutants of Saccharomyces cerevisiae. *J Biol Chem* **1988,** *263* (34), 18118-18122.

48. Perlin, D. S.; Brown, C. L.; Haber, J. E. Membrane potential defect in hygromycin B-resistant pma1 mutants of Saccharomyces cerevisiae. *J. Biol. Chem.* **1988,** *263* (34), 18118-18122.

49. Froschauer, E.; Nowikovsky, K.; Schweyen, R. J. Electroneutral K+/H+ exchange in mitochondrial membrane vesicles involves Yol027/Letm1 proteins. *Biochim Biophys Acta* **2005,** *1711* (1), 41-48.

50. Nowikovsky, K.; Froschauer, E. M.; Zsurka, G.; Samaj, J.; Reipert, S.; Kolisek, M.; Wiesenberger, G.; Schweyen, R. J. The LETM1/YOL027 gene family encodes a factor of the mitochondrial K+ homeostasis with a potential role in the Wolf-Hirschhorn syndrome. *J Biol Chem* **2004,** *279* (29), 30307-30315.

51. Wilkens, S.; Vasilyeva, E.; Forgac, M. Structure of the vacuolar ATPase by electron microscopy. *J Biol Chem* **1999,** *274* (45), 31804-31810.

52. Stevens, T. H.; Forgac, M. Structure, function and regulation of the vacuolar (H+)-ATPase. *Annu Rev Cell Dev. Biol* **1997,** *13,* 779-808.

53. Zhang, Z.; Charsky, C.; Kane, P. M.; Wilkens, S. Yeast V1-ATPase: affinity purification and structural features by electron microscopy. *J Biol Chem* **2003,** *278* (47), 47299-47306.

54. Zhang, J.; Myers, M.; Forgac, M. Characterization of the V0 domain of the coated vesicle (H+)-ATPase. *J Biol Chem* **1992,** *267* (14), 9773-9778.

55. Kawasaki-Nishi, S.; Nishi, T.; Forgac, M. Yeast V-ATPase complexes containing different isoforms of the 100-kDa a-subunit differ in coupling efficiency and in vivo dissociation. *J Biol Chem* **2001,** *276* (21), 17941-17948.

56. Serrano, R.; Rodriguez-Navarro, A. Ion homeostasis during salt stress in plants. *Curr. Opin. Cell Biol* **2001,** *13* (4), 399-404.

57. Sychrova, H. Yeast as a model organism to study transport and homeostasis of alkali metal cations. *Physiol Res* **2004,** *53 Suppl 1,* S91-S98.

58. Soong, T. W.; Yong, T. F.; Ramanan, N.; Wang, Y. The Candida albicans antiporter gene CNH1 has a role in Na+ and H+ transport, salt tolerance, and morphogenesis. *Microbiology* **2000,** *146 (Pt 5),* 1035-1044.

59. Corratge, C.; Zimmermann, S.; Lambilliotte, R.; Plassard, C.; Marmeisse, R.; Thibaud, J. B.; Lacombe, B.; Sentenac, H. Molecular and functional characterization of a Na(+)-K(+) transporter from the Trk family in the ectomycorrhizal fungus Hebeloma cylindrosporum. *J Biol Chem* **2007,** *282* (36), 26057-26066.

60. Rodriguez-Navarro, A.; Sancho, E. D.; Perez-Lloveres, C. Energy source for lithium efflux in yeast. *Biochim Biophys Acta* **1981,** *640* (1), 352-358.

61. Beilby, M. J.; Blatt, M. R. Simultaneous Measurements of Cytoplasmic K Concentration and the Plasma Membrane Electrical Parameters in Single Membrane Samples of Chara corallina. *Plant Physiol* **1986,** *82* (2), 417-422.

62. Blatt, M. R.; Rodriguez-Navarro, A.; Slayman, C. L. Potassium-proton symport in Neurospora: kinetic control by pH and membrane potential. *J Membr. Biol* **1987,** *98* (2), 169-189.

63. Rodriguez-Navarro, A. Potassium transport in fungi and plants. *Biochim. Biophys Acta* **2000,** *1469* (1), 1-30.

64. Calero, F.; Gomez, N.; Arino, J.; Ramos, J. Trk1 and Trk2 define the major K(+) transport system in fission yeast. *J Bacteriol* **2000,** *182* (2), 394-399.

65. Nakamura, R. L.; Gaber, R. F. Studying ion channels using yeast genetics. *Methods Enzymol.* **1998,** *293*, 89-104.

66. Rodriguez-Navarro, A.; Rubio, F. High-affinity potassium and sodium transport systems in plants. *J Exp Bot.* **2006,** *57* (5), 1149-1160.

67. Ko, C. H.; Buckley, A. M.; Gaber, R. F. TRK2 is required for low affinity K+ transport in Saccharomyces cerevisiae. *Genetics* **1990,** *125* (2), 305-312.

68. Gaber, R. F. Molecular genetics of yeast ion transport. *Int Rev Cytol.* **1992,** *137*, 299-353.

69. Mulet, J. M.; Leube, M. P.; Kron, S. J.; Rios, G.; Fink, G. R.; Serrano, R. A novel mechanism of ion homeostasis and salt tolerance in yeast: the Hal4 and Hal5 protein kinases modulate the Trk1-Trk2 potassium transporter. *Mol. Cell Biol* **1999,** *19* (5), 3328-3337.

70. Bertl, A.; Ramos, J.; Ludwig, J.; Lichtenberg-Frate, H.; Reid, J.; Bihler, H.; Calero, F.; Martinez, P.; Ljungdahl, P. O. Characterization of potassium transport in wild-type and isogenic yeast strains carrying all combinations of trk1, trk2 and tok1 null mutations. *Mol Microbiol* **2003,** *47* (3), 767-780.

71. Serrano, R. Halotolerance Genes in Yeast. 2004; pp 491-504.

72. Banuelos, M. A.; Sychrova, H.; Bleykasten-Grosshans, C.; Souciet, J. L.; Potier, S. The Nha1 antiporter of Saccharomyces cerevisiae mediates sodium and potassium efflux. *Microbiology* **1998,** *144 (Pt 10)*, 2749-2758.

73. Prior, C.; Potier, S.; Souciet, J. L.; Sychrova, H. Characterization of the NHA1 gene encoding a Na+/H+-antiporter of the yeast Saccharomyces cerevisiae. *FEBS Lett.* **1996,** *387* (1), 89-93.

74. Watanabe, J.; Uehara, K.; Mogi, Y.; Suzuki, K.; Watanabe, T.; Yamazaki, T. Improved transformation of the halo-tolerant yeast Zygosaccharomyces rouxii by electroporation. *Biosci Biotechnol Biochem* **2010,** *74* (5), 1092-1094.

75. Haro, R.; Garciadeblas, B.; Rodriguez-Navarro, A. A novel P-type ATPase from yeast involved in sodium transport. *FEBS Lett.* **1991,** *291* (2), 189-191.

76. Rodriguez-Navarro, A.; Quintero, F. J.; Garciadeblas, B. Na(+)-ATPases and Na+/H+ antiporters in fungi. *Biochim Biophys Acta* **1994,** *1187* (2), 203-205.

77. Wieland, J.; Nitsche, A. M.; Strayle, J.; Steiner, H.; Rudolph, H. K. The PMR2 gene cluster encodes functionally distinct isoforms of a putative Na+ pump in the yeast plasma membrane. *EMBO J.* **1995,** *14* (16), 3870-3882.

78. Banuelos, M. A.; Quintero, F. J.; Rodriguez-Navarro, A. Functional expression of the ENA1(PMR2)-ATPase of Saccharomyces cerevisiae in Schizosaccharomyces pombe. *Biochim Biophys Acta* **1995,** *1229* (2), 233-238.

79. Tse, C. M.; Levine, S. A.; Yun, C. H.; Brant, S. R.; Pouyssegur, J.; Montrose, M. H.; Donowitz, M. Functional characteristics of a cloned epithelial Na+/H+ exchanger (NHE3): resistance to amiloride and inhibition by protein kinase C. *Proc Natl. Acad. Sci U. S. A* **1993,** *90* (19), 9110-9114.

80. Banuelos, M. A.; Ruiz, M. C.; Jimenez, A.; Souciet, J. L.; Potier, S.; Ramos, J. Role of the Nha1 antiporter in regulating K(+) influx in Saccharomyces cerevisiae. *Yeast* **2002,** *19* (1), 9-15.

81. Jia, Z. P.; McCullough, N.; Martel, R.; Hemmingsen, S.; Young, P. G. Gene amplification at a locus encoding a putative Na+/H+ antiporter confers sodium and lithium tolerance in fission yeast. *EMBO J.* **1992,** *11* (4), 1631-1640.

82. Velkova, K.; Sychrova, H. The Debaryomyces hansenii NHA1 gene encodes a plasma membrane alkali-metal-cation antiporter with broad substrate specificity. *Gene* **2006,** *369*, 27-34.

83. Kinclova, O.; Ramos, J.; Potier, S.; Sychrova, H. Functional study of the Saccharomyces cerevisiae Nha1p C-terminus. *Mol. Microbiol.* **2001,** *40* (3), 656-668.

84. Sychrova, H.; Ramírez, J.; Pena, A. Involvement of Nha1 antiporter in regulation of intracellular pH in Saccharomyces cerevisiae. *FEMS Microbiol. Lett.* **1999,** *171* (2), 167-172.

85. Kinclova, O.; Potier, S.; Sychrova, H. The Zygosaccharomyces rouxii strain CBS732 contains only one copy of the HOG1 and the SOD2 genes. *J Biotechnol* **2001,** *88* (2), 151-158.

86. Papouskova, K.; Sychrova, H. Yarrowia lipolytica possesses two plasma membrane alkali metal cation/H+ antiporters with different functions in cell physiology. *FEBS Lett* **2006,** *580* (8), 1971-1976.

87. Papouskova, K.; Sychrova, H. The co-action of osmotic and high temperature stresses results in a growth improvement of Debaryomyces hansenii cells. *Int J Food Microbiol* **2007,** *118* (1), 1-7.

88. Pribylova, L.; Papouskova, K.; Sychrova, H. The salt tolerant yeast Zygosaccharomyces rouxii possesses two plasma-membrane Na+/H+-antiporters (ZrNha1p and ZrSod2-22p) playing different roles in cation homeostasis and cell physiology. *Fungal. Genet Biol* **2008,** *45* (10), 1439-1447.

89. Iwaki, T.; Higashida, Y.; Tsuji, H.; Tamai, Y.; Watanabe, Y. Characterization of a second gene (ZSOD22) of Na+/H+ antiporter from salt-tolerant yeast Zygosaccharomyces rouxii and functional expression of ZSOD2 and ZSOD22 in Saccharomyces cerevisiae. *Yeast* **1998,** *14* (13), 1167-1174.

90. CONWAY, E. J.; DOWNEY, M. pH values of the yeast cell. *Biochem. J.* **1950,** *47* (3), 355-360.

91. Ramos, S.; Balbin, M.; Raposo, M.; Valle, E.; Pardo, L. A. The mechanism of intracellular acidification induced by glucose in Saccharomyces cerevisiae. *J Gen. Microbiol.* **1989,** *135* (9), 2413-2422.

92. Kresnowati, M. T.; Suarez-Mendez, C.; Groothuizen, M. K.; van Winden, W. A.; Heijnen, J. J. Measurement of fast dynamic intracellular pH in Saccharomyces cerevisiae using benzoic acid pulse. *Biotechnol. Bioeng.* **2007,** *97* (1), 86-98.

93. Castle, A. M.; Macnab, R. M.; Shulman, R. G. Measurement of intracellular sodium concentration and sodium transport in Escherichia coli by 23Na nuclear magnetic resonance. *J Biol Chem.* **1986,** *261* (7), 3288-3294.

94. Gillies, R. J.; Alger, J. R.; den Hollander, J. A.; Shulman, R. G. Intracellular pH measured by NMR: methods and results. *Kroc. Found. Ser.* **1981,** *15*, 79-104.

95. Slavik, J. Intracellular pH of yeast cells measured with fluorescent probes. *FEBS Lett.* **1982,** *140* (1), 22-26.

96. Bracey, D.; Holyoak, C. D.; Coote, P. J. Comparison of the inhibitory effect of sorbic acid and amphotericin B on Saccharomyces cerevisiae: is growth inhibition dependent on reduced intracellular pH? *J Appl. Microbiol.* **1998,** *85* (6), 1056-1066.

97. van Roermund, C. W. T.; de Jong, M.; IJlst, L.; van Marle, J.; Dansen, T. B.; Wanders, R. J. A.; Waterham, H. R. The peroxisomal lumen in Saccharomyces cerevisiae is alkaline. *J. Cell Sci.* **2004,** *117* (18), 4231-4237.

98. Sureshkumar, G. K.; Mutharasan, R. Intracellular pH responses of hybridoma and yeast to substrate addition and acid challenge. *Ann. N. Y. Acad. Sci* **1994,** *745*, 106-121.

99. Miesenbock, G.; De Angelis, D. A.; Rothman, J. E. Visualizing secretion and synaptic transmission with pH-sensitive green fluorescent proteins. *Nature* **1998,** *394* (6689), 192-195.

100. SHIMOMURA, O.; JOHNSON, F. H.; SAIGA, Y. Extraction, purification and properties of aequorin, a bioluminescent protein from the luminous hydromedusan, Aequorea. *J Cell Comp Physiol* **1962,** *59*, 223-239.

101. Inouye, S.; Tsuji, F. I. Evidence for redox forms of the Aequorea green fluorescent protein. *FEBS Lett.* **1994,** *351* (2), 211-214.

102. Prasher, D. C.; Eckenrode, V. K.; Ward, W. W.; Prendergast, F. G.; Cormier, M. J. Primary structure of the Aequorea victoria green-fluorescent protein. *Gene* **1992,** *111* (2), 229-233.

103. Chalfie, M.; Tu, Y.; Euskirchen, G.; Ward, W. W.; Prasher, D. C. Green fluorescent protein as a marker for gene expression. *Science* **1994,** *263* (5148), 802-805.

104. Inouye, S.; Tsuji, F. I. Aequorea green fluorescent protein. Expression of the gene and fluorescence characteristics of the recombinant protein. *FEBS Lett* **1994,** *341* (2-3), 277-280.

105. Kneen, M.; Farinas, J.; Li, Y.; Verkman, A. S. Green fluorescent protein as a noninvasive intracellular pH indicator. *Biophys. J.* **1998,** *74* (3), 1591-1599.

106. Sankaranarayanan, S.; Ryan, T. A. Real-time measurements of vesicle-SNARE recycling in synapses of the central nervous system. *Nat. Cell Biol* **2000,** *2* (4), 197-204.

107. Calahorra, M.; Martinez, G. A.; Hernandez-Cruz, A.; Pena, A. Influence of monovalent cations on yeast cytoplasmic and vacuolar pH. *Yeast* **1998,** *14* (6), 501-515.

108. Kresnowati, M. T.; Suarez-Mendez, C. M.; van Winden, W. A.; van Gulik, W. M.; Heijnen, J. J. Quantitative physiological study of the fast dynamics in the intracellular pH of Saccharomyces cerevisiae in response to glucose and ethanol pulses. *Metab Eng* **2008,** *10* (1), 39-54.

109. Sigler, K.; Kotyk, A.; Knotkova, A.; Opekarova, M. Processes involved in the creation of buffering capacity and in substrate-induced proton extrusion in the yeast Saccharomyces cerevisiae. *Biochim Biophys Acta* **1981,** *643* (3), 583-592.

List of Tables